Coelomogenesis in larvae of *Phoronis ovalis* and *P. muelleri* (Phoronida)

Introduction

The larvae of phoronids possess three distinctive body regions, the preoral hood-like lobe, the postoral tentacle region, and the posterior trunk (Hyman 1959, Zimmer 1964, Emig 1974; 1977). Since the end of the 19th century, the origin of the mesoderm and the mode of coelom formation in Phoronida has been the subject of numerous studies resulting in controversial opinions about its nature (Kowalewsky 1867, Caldwell 1885, Ikeda 1901, Brooks & Cowles 1905, Selys-Longchamps 1907, Zimmer 1964, 1980, Malakhov & Temereva 1999, Bartolomaeus 2001, Freeman & Martindale 2002, Santagata 2004, Temereva & Malakhov 2006). There is general agreement that the process of mesoderm formation occurs in two successive but distinct events: the first one occurs shortly before or immediately after gastrulation, the second phase occurs after the development of mouth and anus (Herrmann 1986, Zimmer 1980). Authors in the late 19th century describe the first mesoblasts to be observed out of line with blastomeres on the ventral side migrating into the blastocoelic space of the coeloblastula (Kowalewsky 1867, Caldwell 1885). The first mesodermal cells in *Phoronopsis harmeri* Pixell, 1912 are derived by ingression of cells from the gastral plate at the beginning of gastrulation (Zimmer 1964). In *Phoronis muelleri* Selys-Longchamps, 1903 the mesoderm separates with many cells simultaneously from the epithelium of the vegetal side (Herrmann 1980) of the gastrula. This mode of initial mesoderm formation occurs also in *P. vancouverensis* Pixell, 1912 [sub *P. vancouverensis*, according to Emig 1971] and *P. ijimai* Oka, 1897 (Ikeda 1901, Zimmer 1964). The majority of these authors come to the conclusion that the second phase of mesoderm formation occurs mostly on the anterior and/or lateral sides of the blastopore at the time of fusion of the blastoporal lips (for an overview see Zimmer 1964, Emig 1974, 1977). Malakhov & Temereva (1999) as well as Freeman & Martindale (2002) describe in a recent study of the development of *P. ijimai* the second phase of mesoderm formation to occur at the ectoderm/endoderm boundary, at the connection of the mouth with the ectoderm as well as at the connection of the anus with the ectoderm.

The number of coelomic compartments recognized for the phoronids and their larvae closely conforms to the theory of archimeric segmentation, suggested by Masterman (1898) that he based on the results of Sedgwick (1886). Masterman (1898) states that the somites of segmented animals are derived from endodermal pouches, and that they were homologous

to gastric cavities found in coelenterates. Although it could never be confirmed that the mesoderm in Phoronida derives from endodermal pouches, some of the findings as for instance the paired coelomic cavities in triploblastic coelomate bilateria (Masterman 1898, 1900) gained further support by the study of Zimmer (1964). The latter author claimed the existence of a coelomic lining in the anterior hood of the actinotroch larvae of *P. ijimai*, thus forming a protocoel, comparable to the protocoel found in echinoderms and enteropneusts. This theory is still controversially discussed and is known as the "archicoelomate concept" (Reisinger 1972, Siewing 1973, 1974b, 1980a, Emig & Siewing 1975, Emig 1976, Pross 1980, Herrmann 1980, 1997).

The main problem arises in the discrimination of coelomic cavities. By definition a coelomic cavity (i.e. secondary body cavity or true coelom) is completely lined by an epithelium - in contrast to a primary body cavity that is always lined by an extra cellular matrix (Bartolomaeus 2001). Two criteria can be elaborated for the existence of an epithelial lining in a coelom cavity: the cells are connected to the basal lamina and they must build a complete epithelium of polarized cells, which are interconnected with neighboring cells by apical adherence junctions. These criteria differentiate the coelom from cavities containing solitary cells or compact masses of mesenchymatous cells. The extracellular matrix, on which the lining cells rest, can be very delicate (ca. 20-50 nm thin) in Phoronida (Bartolomaeus 2001). The presence of any cell-cell connections or cell-matrix connections can hardly be seen at the level of light microscopy. The recognition of a body space as a coelomic cavity is difficult in the phoronids, as both primary and secondary body cavities occur at the same time. This results in controversial discussions, whether the hood cavity for instance is completely lined by cells, thus forming a true coelom, or whether it contains isolated cells or even no cells (see Zimmer 1964:272f for an overview).

Recent studies at ultra structural level have shown that in the development of brachiopods and phoronids, there is never a separate, completely lined coelomic cavity in the anterior body of the larvae (Lüter 1998, 2000, Grobe, 2000, Bartolomaeus 2001). Among brachiopods, the coelom in *Novocrania anomala* (Müller, 1776) develops from a single anlage, resulting in two coelomic cavities (Grobe 2000, Grobe, Lüter & Bartolomaeus in prep.). The same can be observed in the articulate brachiopods *Notosaria nigricans* (Sowerby, 1846) and *Calloria inconspicua* (Sowerby 1846, Lüter 1998, 2000). The preoral hood of the larva of *P. muelleri* is entirely filled with a presumably gel-like matrix and contains no coelomic cavity (citation). Thus, only two coelomic cavities, the tentacle coelom and the trunk coelom, are present in phoronids (Bartolomaeus 2001). In adult *P. ovalis* Wright, 1856 the coelomic lining of the epistome constitutes a continuous epithelium with the lining of the tentacle coelom (Gruhl *et al.* 2005). Therefore the epistome of *P. ovalis* could not be

considered to possess a separate coelom ("Protocoel").

Until now, no ultrastructural examinations dealing with the origin of the mesoderm in Phoronida exist. Moreover, except for the description of the outer development (Silén 1954), the larval development of *P. ovalis* is completely unknown. The present study provides first insights in the ultrastructure of the mesoderm formation in *P. muelleri* and *P. ovalis* and the fate of the coelomic anlage in *P. ovalis*.

Material and Methods

Phoronis ovalis lives in tubes in the outer shell-layers of empty Bivalvia. By transverse fission a regular network of several specimen is build in one shell.
Empty bivalve shells of *Modiola modiolus* (mollusca) were dredged along a line between 58º 13'N, 11º 24'E and 58º 12'N, 11º 24'E in the waters off Kristineberg (Sweden) in November 2000 at a depth of 36 to 37 m. The shells containing specimens of *P. ovalis* were kept in laboratory under running seawater at 17° C.
During this time of the year almost every tube of the phoronids contains larvae (Silén 1954). By breaking the shells numerous tubes of the phoronids are opened and the larvae contained in these tubes, are released. The larvae from one individual tube are approximately at the same stage of development, but differ from the ones in other tubes. This indicates that the fertilization in one individual takes place at the same time (Silén 1954).
The larvae had completed gastrulation but were not older than the stage described by Silén (1954: Fig. 21), thus indicating that the larvae are brooded until this time in the tube of the adult and liberated at a later stage, not like Silén (1954) assumed, released in an advanced gastrula stage (his figure 18).
To study the formation of the mesoderm and the coelomogenesis, larvae at different stages of development were collected from the tubes of the adult specimen. The larvae were fixed in 2.5% glutaraldehyde (grade I, 25% in H_2O, Sigma-Aldrich, Germany), buffered in sodium cacodylate at 970 mOsm, pH 7.2 at 4° C. The fixation was stopped after 20 min followed by several rinsing procedures with sodium cacodylate, 970 mOsm, pH 7.2 at 4º C. Post fixation was carried out with 2% Osmium tetroxide buffered in 0.1 M sodium cacodylate. To stain matrix components, Ruthenium red and Alcian blue had been added to the fixative (Crawford 1989).
For scanning electron microscopy the larvae were dehydrated in graded series of acetone up to 100%, critical point dried with CO_2 in a Bal-Tec CPD 030 and subsequently sputter coated with gold with a Bal-Tec SC 005. The larvae were examined in a Leo VP 450 SEM at 60 kV (Philips Electron Optics, Netherlands) at the Free University of Berlin.

For transmission electron microscopy the larvae were treated in the same manner up to 100% acetone, transferred to into propylene oxide and embedded in araldite. Silver interference colored sections (60-70 nm) were cut on a diamond knife, stained with uranyl acetate and Reynold's lead citrate.

Phoronis muelleri lives in tubes in soft substrate. Adult specimens of *P. muelleri* were dredged from the "Phoronis Grund" off Heligoland/Germany in a rectangle described by the following coordinates: 54º 10'N, 7º 42'E; 54º 08'N, 7º 42'E; 54º 10'N, 7º 47'E; 54º 8'N, 7º 47'E in the end of July 2003.

Ripe eggs in females are located in the trunk coelom between ampullae and lophophore. The lophophores of animals were removed with fine scissors and the eggs collected in a 50 ml glasbowl with a glass pipet. Sperm was taken directly from the gonads of ripe males located in the ampulla of the animal. After fertilization the eggs undergo total and regular cleavages with a mean cell cycle of 35 min at 10º C. After 10 to 17 h ciliated blastula-stages have been developed. The culture medium used was taken from seawater from the house-owned aquaria at the Heligoland aquaria, filtered through Sartorious 0.2 µm Nalgene-filter and autoclaved at 140º C for 1 h.

Successive stages starting from early gastrula (30 h post fertilization) until 4 d 15 h post fertilization (PF) were fixed for 30 min and prepared for transmission and scanning electron microscopy as described for *P. ovalis*, except that the cacodylate buffer had been replaced by 0.1M PBS.

The different developmental stages of *P. ovalis* and *P. muelleri* were examined in a Philips CM 100 transmission electron microscope (Philips Electron Optics, Netherlands) at 60 kV. Pictures were recorded on Ditabis negative plates (Digital Biomedical Imaging Systems AG, Germany), directly scanned with the Ditabis micron reader into a 16 bit IPL-format and converted with Analysis 3.0 (Soft Imaging System, Germany) into 8 bit tiff files.

Virtual 3D representations were reconstructed by taking pictures from complete series of cross- and sagittally sectioned larvae every 10th or 20th section. The image series were aligned in Photoshop 9.0 (Adobe Systems Inc., USA) and reconstructed by building polygon models with NURMS smoothing in 3d Studio Max 6.0 (Autodesk Inc., USA).

Terminology

The different larval stages of *P. ovalis* are recognized according to conspicuous external characters. These characters include the ciliation, the development of mouth and anus, the opening of the nephropori, and the beginning of muscular movement. The terminology for this larva follows the one introduced by Silén (1954).

The terms "trunk" and "lophophore" are used instead of "metasome" and "mesosome". Accordingly the names of the corresponding coelomic cavities, trunk coelom and lophophore coelom are applied (see Gruhl *et al.* 2005).

Results

Coelomogenesis in *Phoronis ovalis*

Overview

The youngest embryos collected from opened tubes are in the stage of a late blastula and are of a flattened ovoid shape. The most advanced developmental stages in the tube are approximately box-shaped with mouth and anus situated in the ventral midline. In these stages the entire ventral side is made up of a tall epithelium, which functions as a creeping sole, allowing the embryo slow creeping movements (Fig. 6).

The origin and formation of the mesoderm in the larva of *P. ovalis* can be traced back to the time of the late blastula stage. Within the flattened shape of the embryo the blastocoel forms a narrow slit-like space. First precursors of mesodermal cells originate from the centre of the vegetal side by delamination of eight cells (Fig. 1). These cells are seen as single spherical cells in the blastocoelic space (Fig. 2 B, C). Gastrulation occurs by invagination of blastomeres in the midventral surface, resulting in a wide blastopore opening into the archenteron, which completely obliterates the blastocoelic space. The future lumen of the digestive system can be traced back to slit-like spaces between the endodermal cell mass. The tip of the archenteron is situated in close contact with the anterior ectoderm (Fig. 3). Prospective mesodermal cells appear at this stage in the cell mass on the vegetal side on both sides of the archenteron (Fig. 3 A). These cells are undifferentiated and form a compact strand of cells (Fig. 3 A). This compact strand of cellsgrows dorsad between the sheets of ecto- and endoderm (Fig. 4). At this late gastrula stage the blastopore, which will later form the mouth, opens into the blindly ending archenteron. Posterior to the Blastopore an opening is located, which will later form the anus. It opens into a short proctodeum, which ends blindly in the posterior centre of the body (Fig. 5). At the same time as the anus is formed, a pair of protonephridia is developed in the ectoderm on both posterior-lateral sides of the larvae.

The initial anlage of mesodermal cells becomes divided into two compartments, resulting in one anterior and a smaller, posterior compartment encircling the greater part of the intestine (Fig. 5). The intestinal cells are monociliated and are equipped with a dense bordering of microvilli. The proctodaeum and the anterior intestine are still not connected. A small slit in the endodermal cell mass shows the prospective lumen of the digestive tract (Fig. 8).

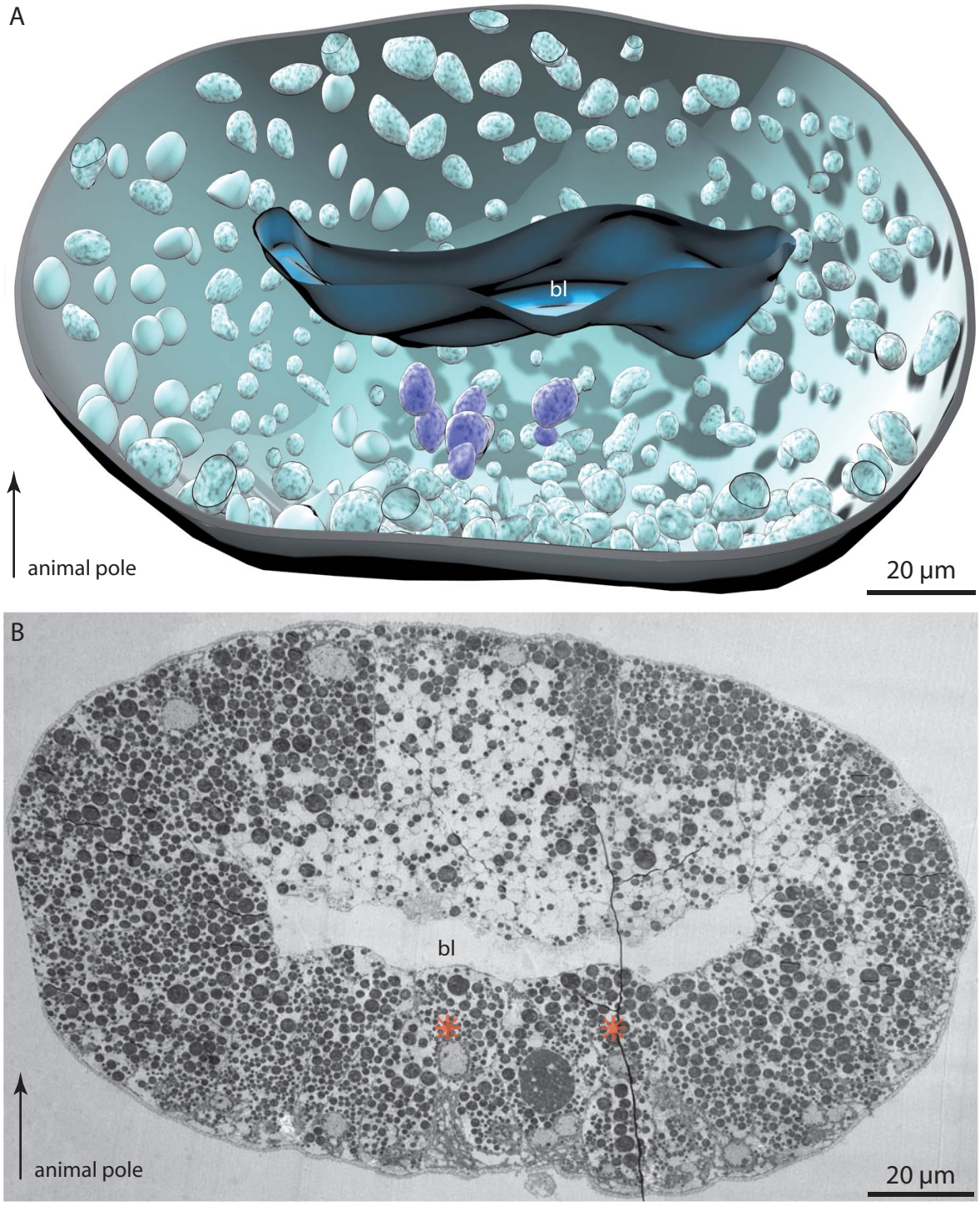

Fig. 1: *P. ovalis*, late blastula stage. **A** Reconstruction of the whole embryo, showing the inner blastocoelic space (*bl*) and the distribution of the nuclei in the blastomeres (turquoise) as well as the nuclei of eight delaminated cells (blue). **B** TEM section near the center, showing delaminated cells (*red asterisks*) embedded between the blastomeres of the vegetal pole.

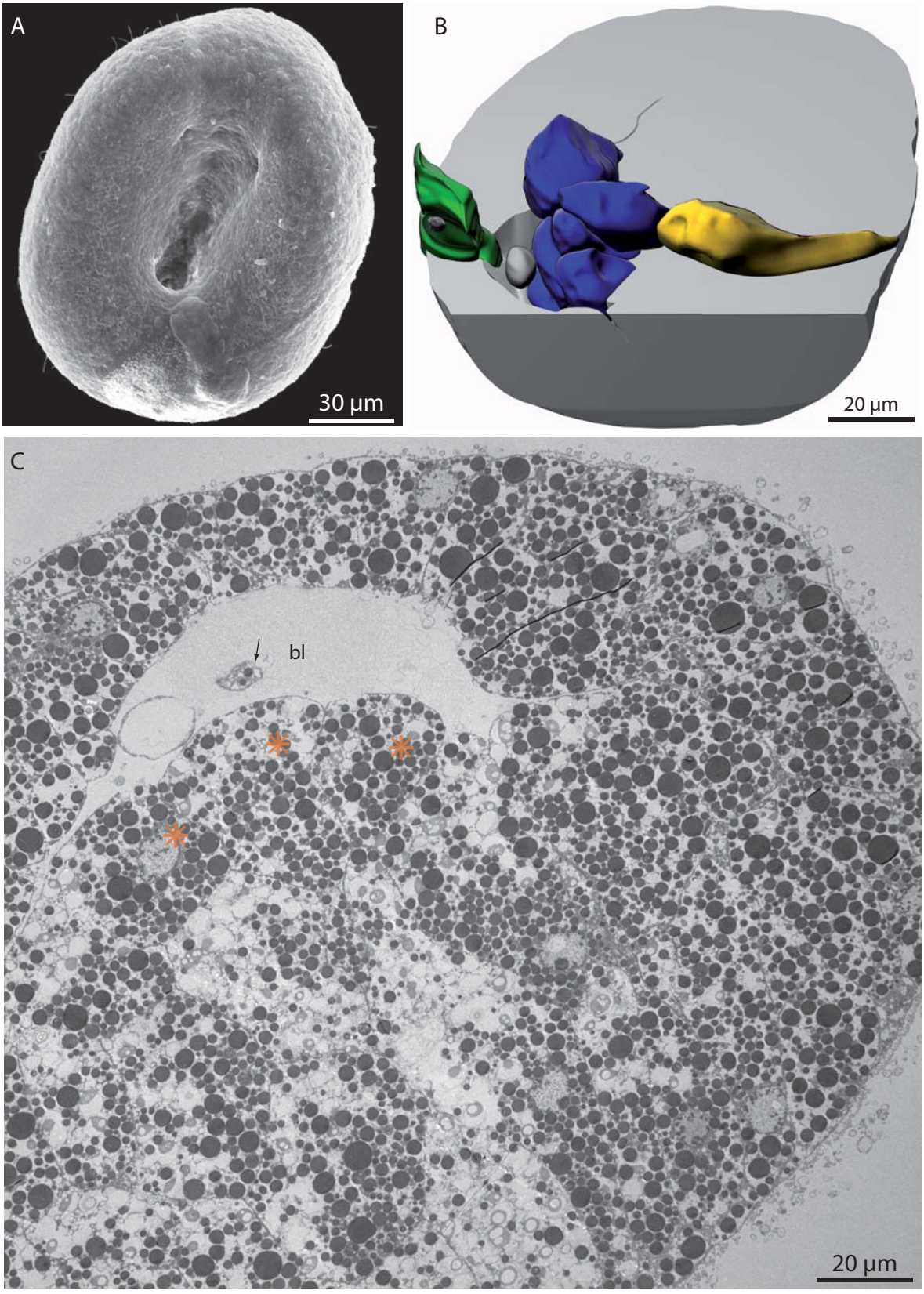

Fig. 2: *P. ovalis*, late blastula and gastrula stage. **A** SEM micrograph of the gastrula with the broad blastopore; which is longitudinal stretched. The archenteron is deeply invaginated. **B** 3D-reconstruction (longitudinal) of the late blastula stage. Blastomeres at the vegetal pole are shaded yellow, on the animal pole green, and mesoblasts inside the blastocoelic space are shaded blue. The remaining ectodermal cells of the embryo are shaded gray. **C** Longitudinal TEM section through mesoblasts (*asterisks*). A single cell is situated in the blastocoel (*bl*) (*arrow*, also gray cell in B). Note: there is no ECM separating both the cells from the vegetal pole and the mesoblasts.

Gastrulation

The flattened ovoid embryo shortly before gastrulation is 500 µm long, 180 µm broad and measures 140 µm along the animal-vegetal axis. The blastula is yellow and opaque, SEM-examinations reveal short cilia, growing on the surfaces of the cells and covering the surface uniformly (Fig. 2 A). The ventral area of the embryo is slightly concave indicating the site of gastrulation.

The blastomeres are long and columnar in cross sections; as a result, the blastocoelic space is flattened to a narrow slit. The outer apical surfaces of the blastomeres possess a dense border of microvilli. All cells contain a high amount of yolk vesicles in the form of electron dense staining, large spheres. In the blastomeres forming the vegetal pole the yolk vesicles are evenly distributed, at the animal pole the most yolk granules are restricted to the outer (apical) part of the cytoplasm (Fig. 1 B). The basal part of the blastomeres at the animal pole oriented towards the blastocoelic space contains few yolk vesicles but numerous electron light vesicles. The nuclei of all blastomeres are located in the apical side of each cell (Fig. 1).

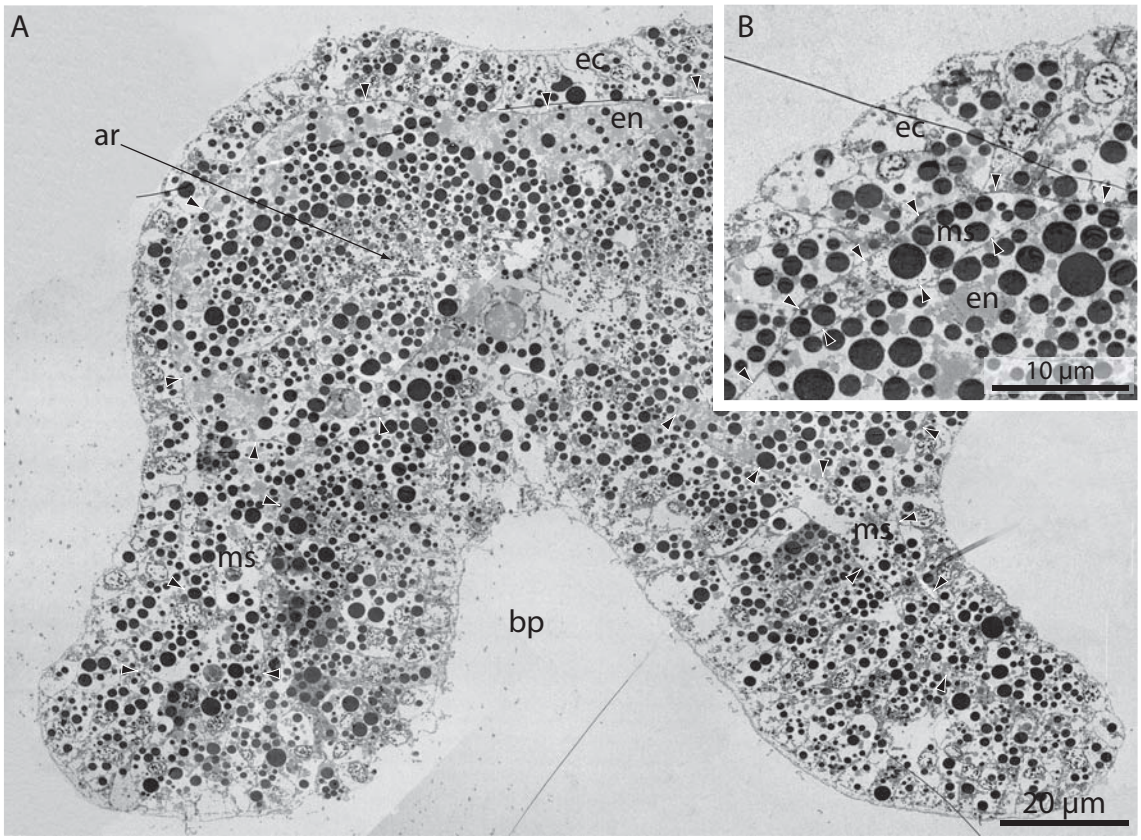

Fig. 3: *P. ovalis*, late gastrula. **A** Midsagittal TEM section with monolayered ectoderm (*ec*), strands of mesoderm (*ms*) on both sides of the blastopore (*bp*) and endoderm (*en*). *ar:* extension of lumen of the archenteron in the endoderm. All three layers are separated by a thin ECM (*arrowheads*). **B** First mesoderm cells occur on the apical pole enclosed by the ECM of the Ecto- and Endoderm (*arrowheads*).

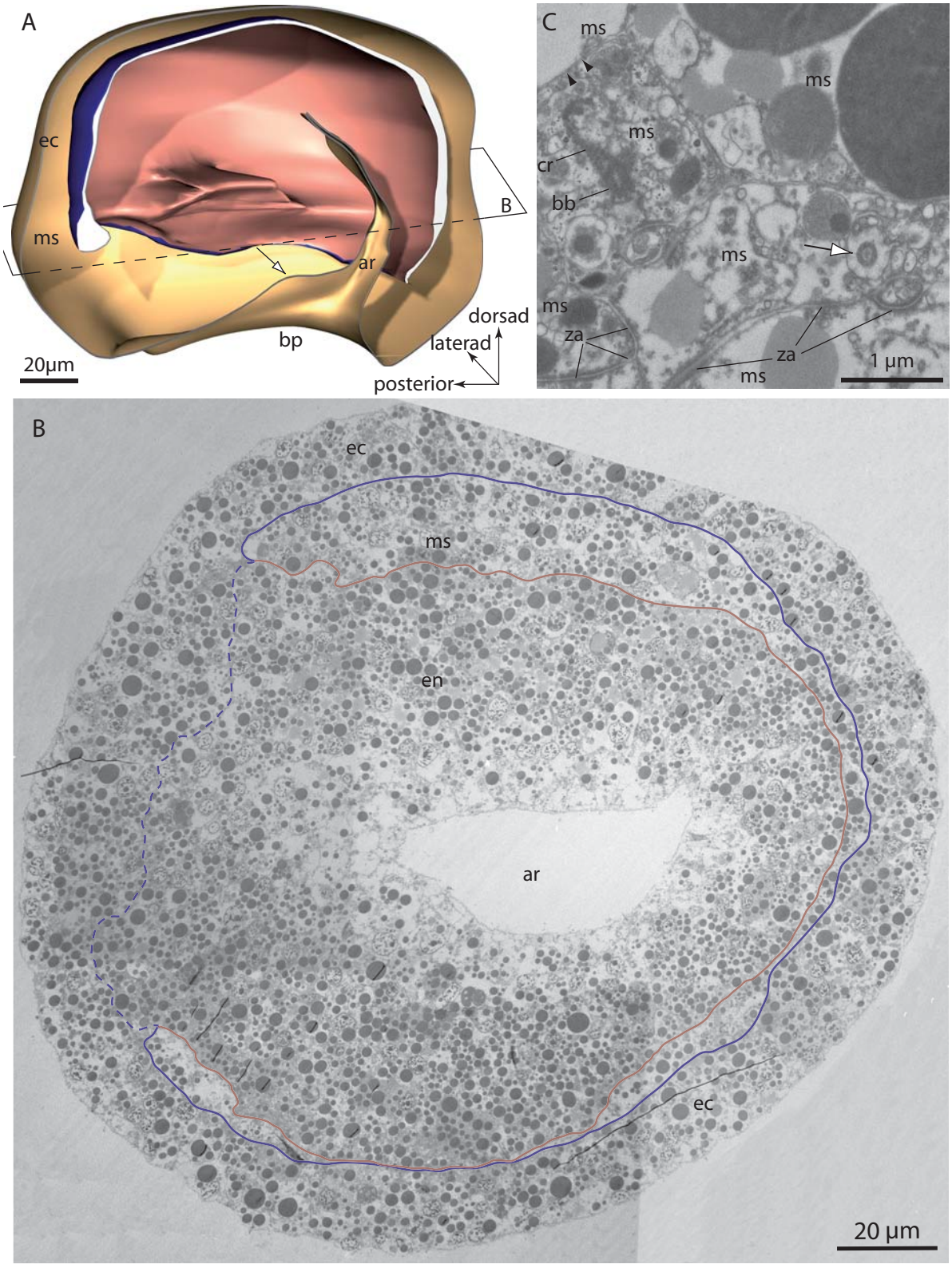

Fig. 4: *P. ovalis*, young larva. **A** Midsagittal section of 3D-drawing of the larva reconstructed from serial TEM sections. The invaginated archenteron (*ar*) narrows to a slit in the center of the larva. In the dorsal wall of the archenteron a small impression shows the place of the invagination of the proctodeum (*arrow*). The prospective mesoderm (*ms*) encloses the endoderm and is pressed into the endoderm on both the lateral sides. **B** Slightly oblique cross section at the level indicated in A, showing the prospective mesoderm surrounding the archenteron. **C** Detail of epithelialisation in the mesodermal cell mass with cilia (*arrow*) already developed and protruding in the expanding lumen. The cells of the mesoderm are connected to the basal lamina by spot desmosomes (*arrowheads*). *bb:* basal body, *bp:* blastopore, *cr:* ciliary rootlet, *ec:* ectoderm, *za:* zonula adherens.

At this stage, only a few blastomeres undergo mitosis at the same time. At the most, two mitotic cells are found in a single embryo. Two cells, smaller than the surrounding blastomeres, are present in the vegetal side of the blastula. They are identical in their cytoplasmatic contents with the remaining vegetal blastomeres, but differ in their positions compared to them: whereas most of the vegetal cells rest on the ECM with their basal poles and build the outer surface of the embryo with their apical poles, the two peculiar smaller cells have no contact to the outside, but rest on the ECM as well. A short time later eight similar cells can be observed, again differing from the remaining blastomeres of the vegetal side by their positions only (Fig. 1 A). This accumulation of cells on the vegetal side of the embryo proceeds, while the epithelial blastomeres on this pole elongate, and the blastomeres on the apical pole shorten (Fig. 2 B, C). A single cell was observed inside the blastocoelic space (Fig. 2 B, C).

Gastrulation results in a deeply invaginated archenteron and a wide open blastopore (Fig. 2 A). After gastrulation is completed, the larva acquires a box-like shape with the lips of the blastopore-opening drawn out to the lateral sides forming a distinct rim around the mouth opening. In sagittal TEM-sections, the late gastrula consists of a monolayered outer ectoderm as well as an underlying endoderm, both separated by a thin basal lamina (25-28 nm thick). On the ventrolateral sides of the blastopore a strand of cells is formed, enclosed by a thin extracellular matrix (ECM). This ECM separates the prospective mesodermal cells completely from the surrounding epithelial cells of the archenteron and the ectoderm (Fig. 3). The cells of this prospective mesoderm form a double layer. The single cells are unpolarized, in the way that they have no zonula adherens as intercellular connections or apical cilia developed.

Young larva

The box-shaped larva becomes ovoidal, the blastopore persists as the mouth opening on the ventral side. From the outside, the young larva shows no further differentiation.

Starting from the compact ring of prospective mesodermal cells now encircling the blastopore, the cell sheet grows dorsad between the layers of ectoderm and endoderm (Fig. 4 A), separated from both by a thin ECM, forming a single-layered cell sheet. Cell growth is not equal over the whole area around the blastopore: anterior there are only few cells, whereas the posterior part reaches nearly up to the dorsal tip of the endoderm. The prospective lateral mesoderm is thickened in the middle part of the body and compressed to a thin sheet by the cell mass of the endoderm (Fig. 4 A). On the lateral side the double-layered strand of cells starts forming an epithelium: basally the cells are connected to the ECM by hemidesmosomes, apically they are interconnected with neighboring cells by zonulae

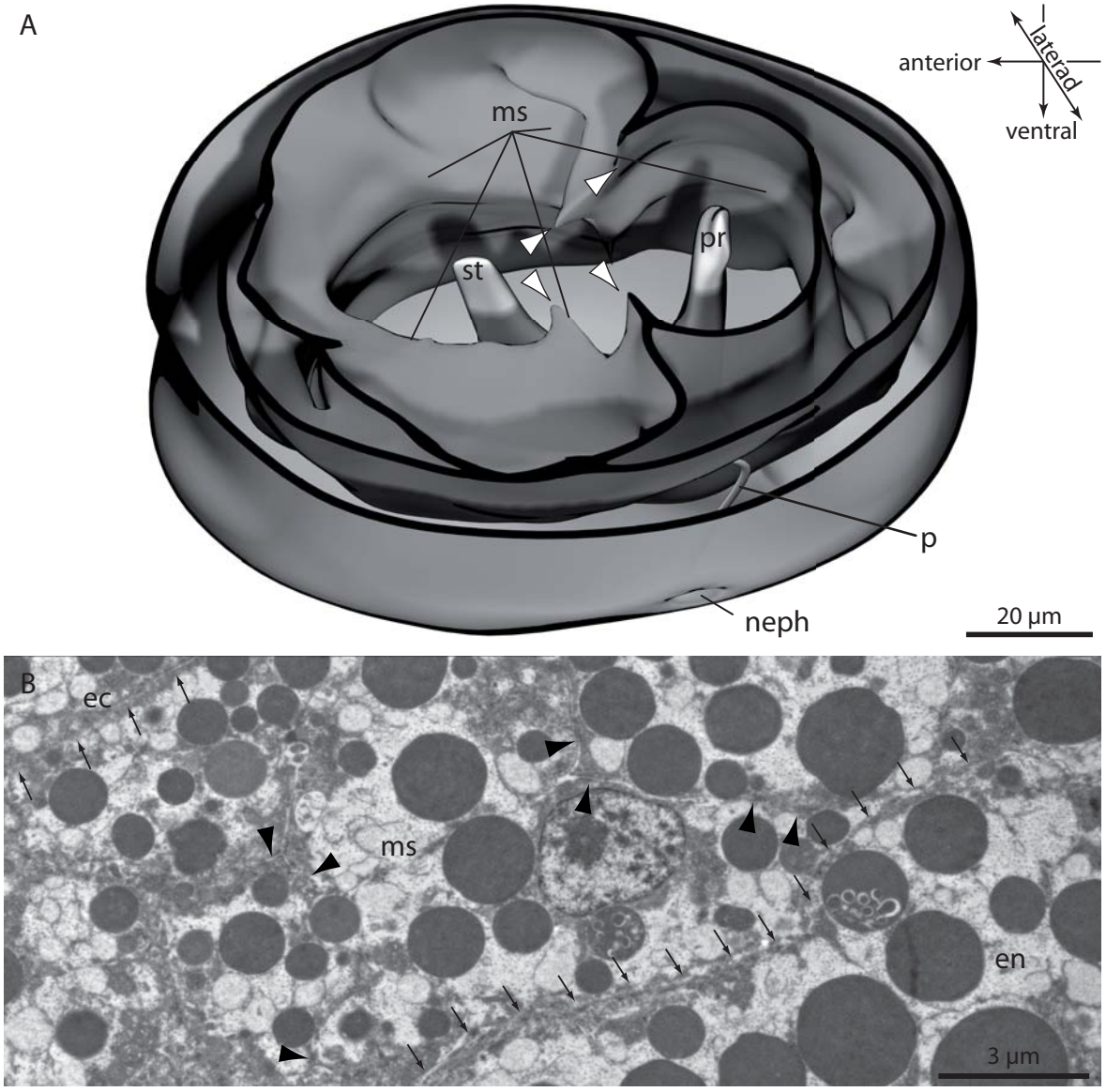

Fig. 5: *P. ovalis*, young larva. **A** Median cross section through 3d reconstruction from serial TEM sections. The mesodermal cell mass surrounding the stomodeum (*st*) and the now invaginated proctodeum (*pr*) is pressed into the endodermal cell mass between the stomodeum and proctodeum (*arrowheads*). Protonephridia (*p*) are located ventrolateral, opening through the nephroporus (*neph*) to the outside. **B** Detail of the mesoderm around the endoderm. It is separated by extracellular matrix from the ectoderm (*ec*) and endoderm (*en*) (*arrows*). Intercellular spaces between the cells are limited by intercellular junctions on the apical side of the cells (*arrowheads*).

adherentes, thus showing an epithelial cell arrangement. A small space occurs between the apical sides of these mesodermal cells, the coelomic lumen. Each of these cells has developed a single cilium (Fig. 4 C). The cilium is anchored in the cytoplasm by one striated rootlet and a basal body, from which nine peripheral microtubuli doublets as well as one central microtubuli-dublett originate, thus showing a 9×2+2 microtubuli pattern of the axoneme. Besides this small coelomic space there are no other intercellular lumina and the blastocoelic space is completely obliterated. At ultrastructural level, the cytological appear-

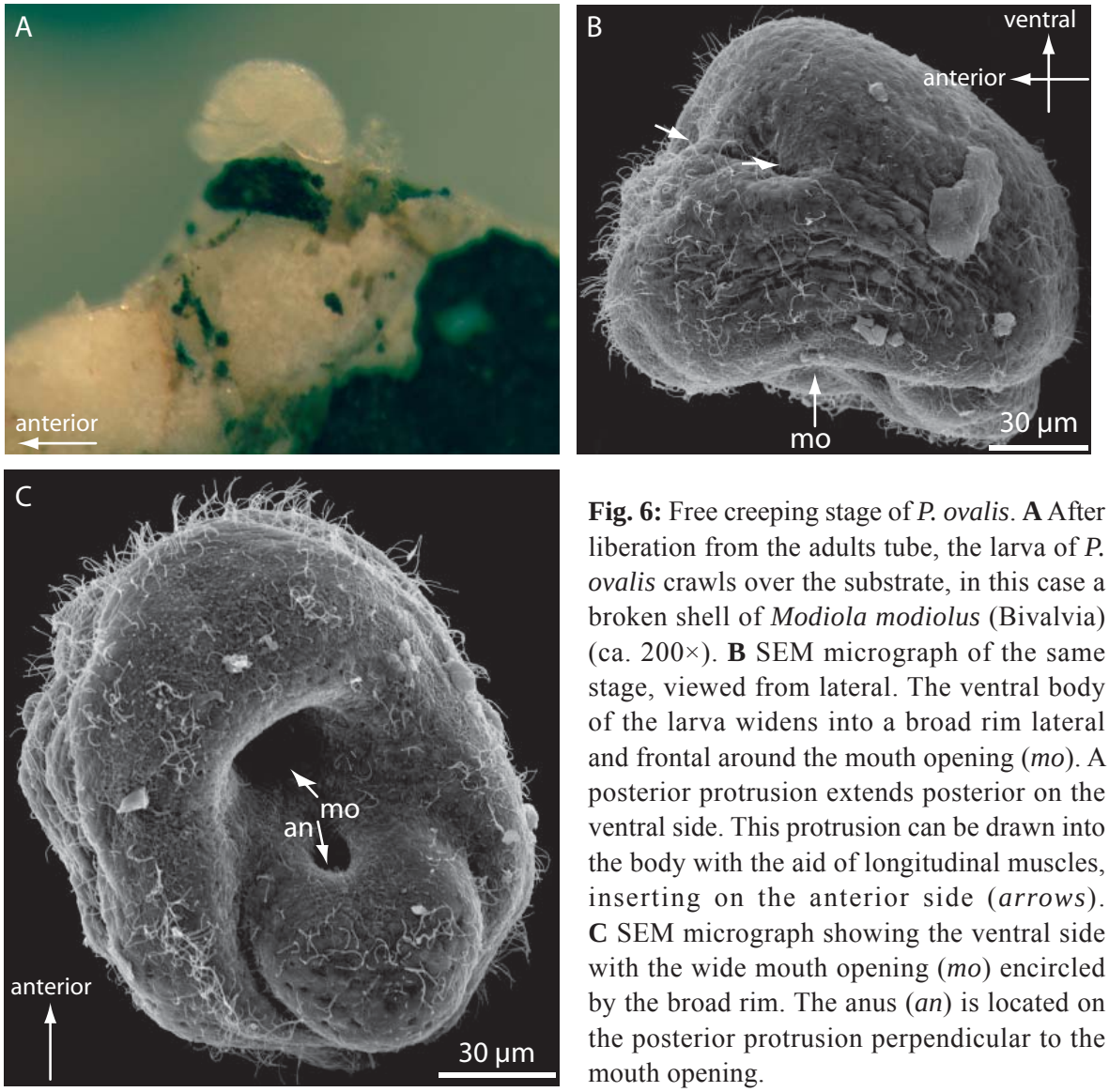

Fig. 6: Free creeping stage of *P. ovalis*. **A** After liberation from the adults tube, the larva of *P. ovalis* crawls over the substrate, in this case a broken shell of *Modiola modiolus* (Bivalvia) (ca. 200×). **B** SEM micrograph of the same stage, viewed from lateral. The ventral body of the larva widens into a broad rim lateral and frontal around the mouth opening (*mo*). A posterior protrusion extends posterior on the ventral side. This protrusion can be drawn into the body with the aid of longitudinal muscles, inserting on the anterior side (*arrows*). **C** SEM micrograph showing the ventral side with the wide mouth opening (*mo*) encircled by the broad rim. The anus (*an*) is located on the posterior protrusion perpendicular to the mouth opening.

ance of the mesodermal cells is similar to the ectoderm and endoderm cells (Fig. 4 B). The large amounts of electron dense staining yolk vesicles form the most obvious content of the cytoplasm. The apical part of the endodermal cells contains numerous electron lucent vesicles. The nuclei are spherical with condensed heterochromatin, distributed throughout the nucleus (Fig. 4 B). Mitochondria and multivesicular bodies are located in the basal parts of the cells.

The anus invaginates through in the posterior wall of the archenteron (Fig. 4 A *arrow*) and forms a protodaeum in the endodermal cell mass. In later development the lateral bulges of the mesoderm on both sides of the larva become more obvious (Fig. 5 A *arrowheads*). The yolk is still homogenously distributed throughout the larva and the electron light vesicles are now not only restricted to the apical parts of the endodermal cells, but are also found in the mesodermal and ectodermal cells. Each cell of the epidermis bears a single, fully developed

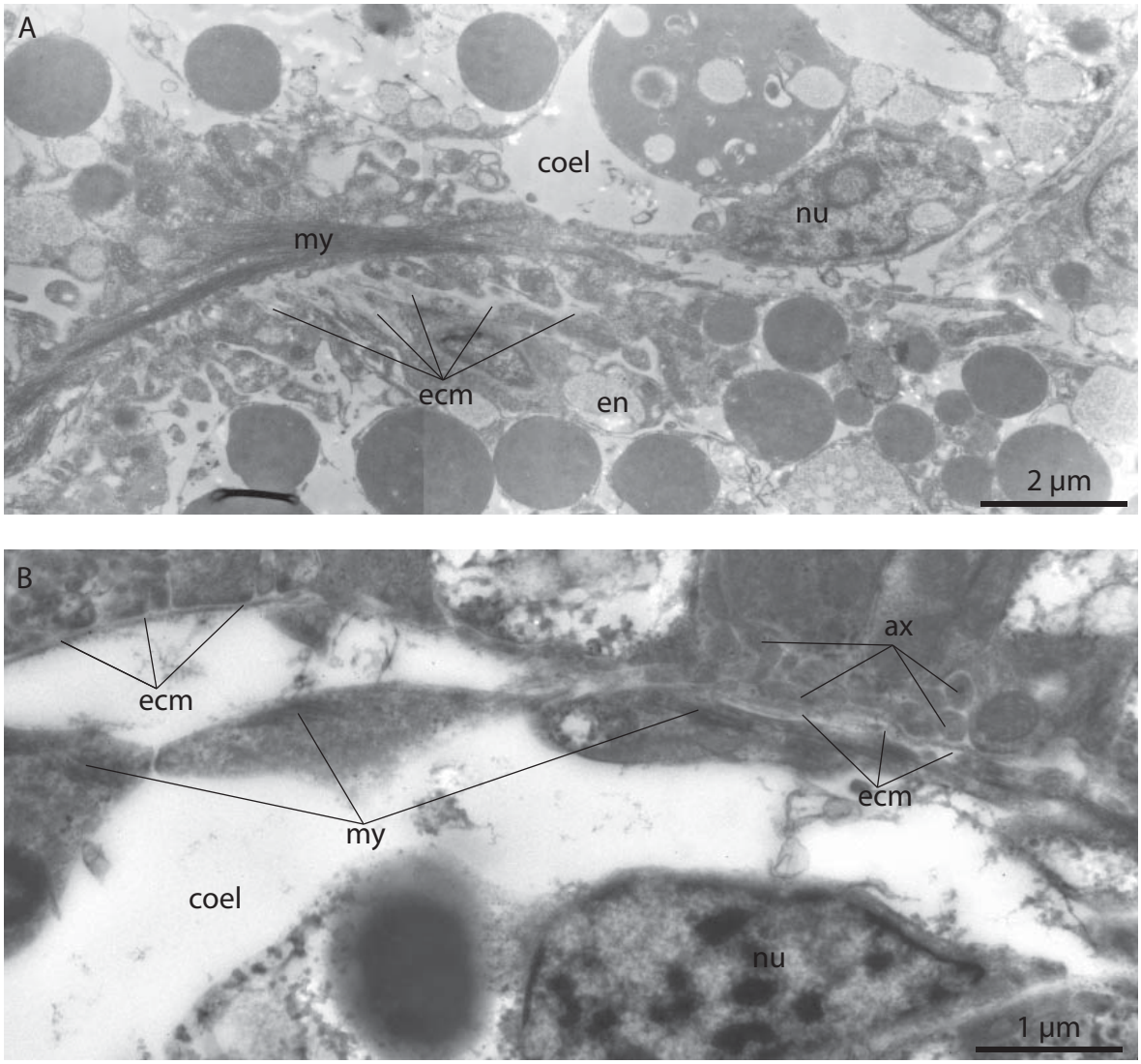

Fig. 7: *P. ovalis*, free creeping stage. **A** Muscle cells resting on the ECM (*ecm*) of the visceral side are anchored in the matrix by cytoplasmatic protrusions. **B** Epitheliomuscle cells lining the visceral ECM of the coelom. *ax*: axon of the neuropil, *coel*: coelom, *en*: endoderm, *my*: myofilaments, *nu*: nucleus.

cilium. Mouth and anus are formed, although they are not connected to each other. The mesodermal strand around the prospective digestive tract is characterized by extensive intercellular spaces. They occur in the posterior region between several cells, which stain dark due to many free ribosomes in their cytoplasm. All of these mesodermal cells have a cilium developed that faces the coelomic cavity. The intercellular spaces between the mesodermal cells are sealed by apical junctions (Fig. 5 B *arrowheads*). The nucleus is situated central within each mesodermal cell. At the same time, a pair of nephridia forms as invaginations of the ectoderm on the ventral sides in the posterior part of the animal (Fig. 5 A).

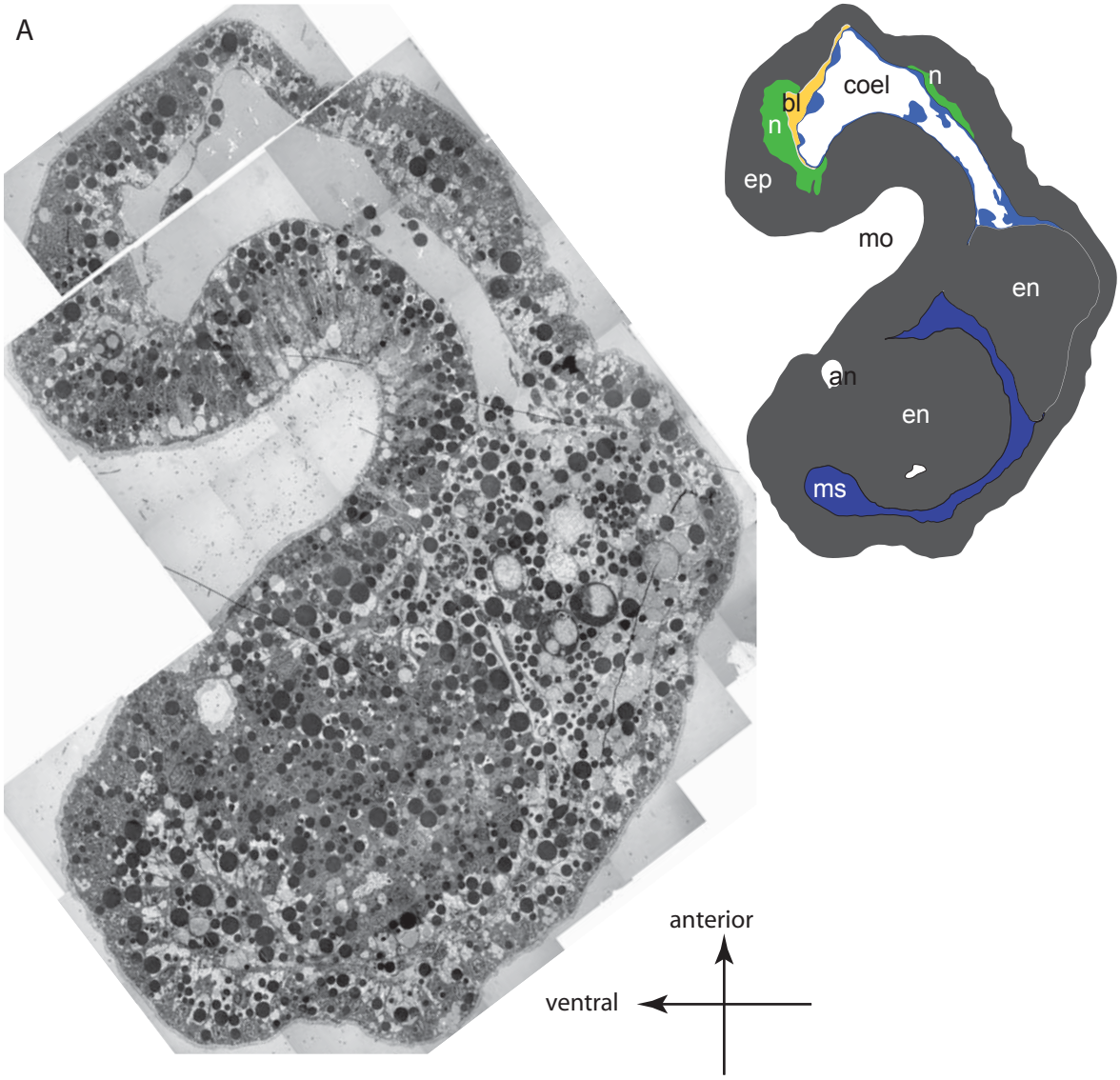
A
coel
n
bl
n
ep
mo
en
an
en
ms
anterior
ventral

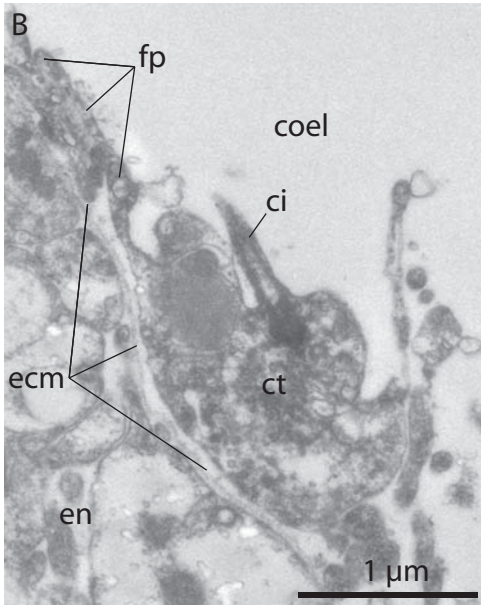
B
fp
coel
ci
ecm
ct
en
1 µm

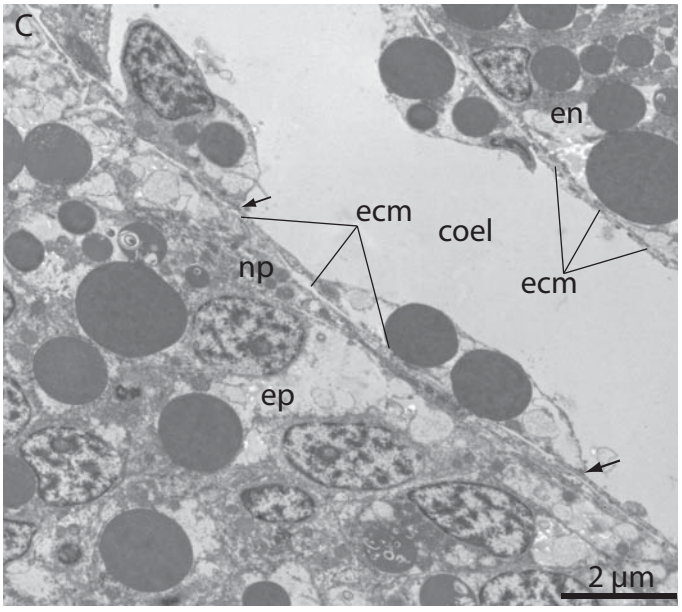
C
en
ecm
coel
np
ecm
ep
2 µm

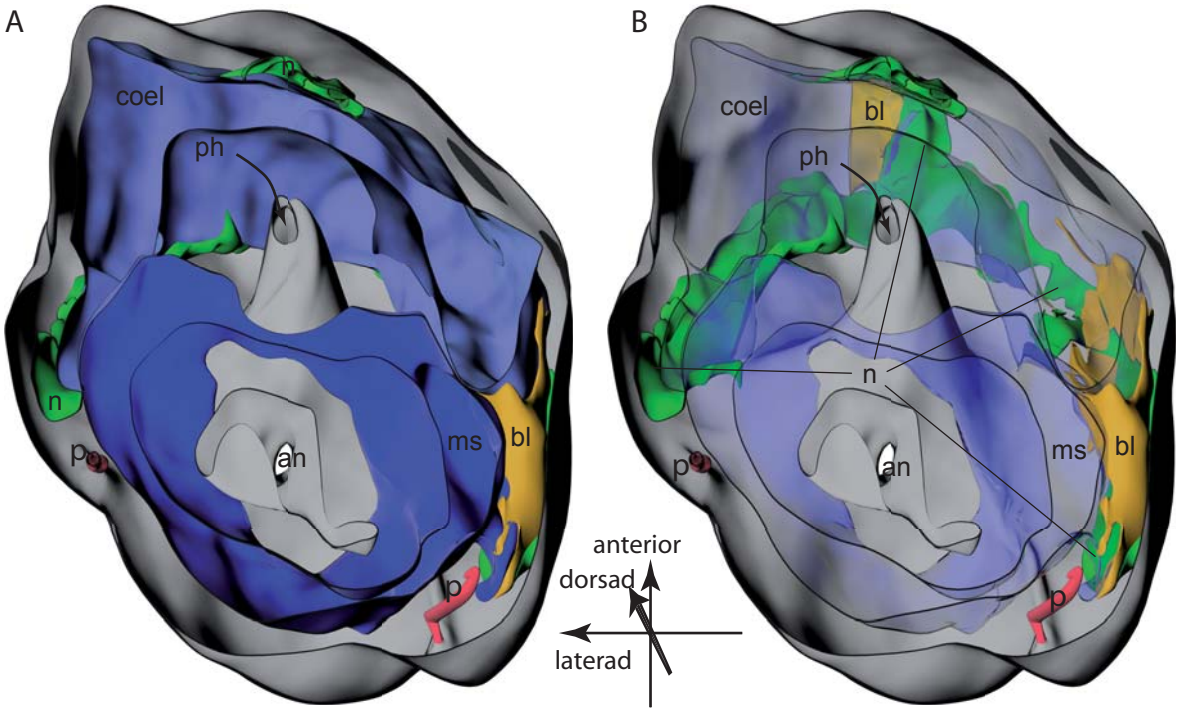

Fig. 9: Free crawling stage larva of *P. ovalis*, ca. three days old. 3D reconstruction from serial ultrastructural sections. View from dorsal into the ventral body. **A** The pharynx (*ph*) is surrounded by the anterior coelom (*coel*) and the posterior compact mesoderm (*ms*), the latter encircling the anus (*an*) as well as prospective intestine completely. Protonephridia (*p*) are located posterior to the anus (*an*). **B** same drawing as A with the coelom and mesoderm transparent, to reveal the position of the blastocoel (*bl*) and the neuropil (*n*). Note how the nephridium is pushed into the mesoderm/ blastocoel on the right side of the larva.

Late larva

The late larva – corresponding to the stage three days after liberation according to Silén (1954, Fig. 21) - is characterized by an extension of the anteroventral rim around the mouth opening and a dense ciliation covering the whole body. At the same stage, a posterior midventral extension is formed perpendicular to the ventral surface out of the body. The anus is situated on the anterior side of this extension (Fig. 6). The larva is capable to crawl slowly over the substrate.

Two large cavities are situated around the prospective digestive tract. Both cavities are lined by a monolayered coelothel. The cells of this coelothel rest either on the subepidermal or on

Fig. 8: Free crawling stage larva of *P. ovalis*, ca. three days old. **A** Longitudinial TEM micrograph: The coelom (*coel)* is separated in an anterior and a posterior compartment. The latter contains an accumulation of mesodermal cells, situated in the ventral wall of the coelothel. **B** Coelothel cell (*ct*) lining the visceral ECM (*ecm*) containing a cilium (*ci*). **C** The coelomic lining is complete and consists of cuboid cells with filamentous processes (*fp*) which overlap each other and are interconnected via adhaerens junctions (*arrows*). *an*: anus, *en:* endoderm, *ep*: epidermis, *n*: neuropil, *mo*: mouth opening, *ms*: mesoderm.

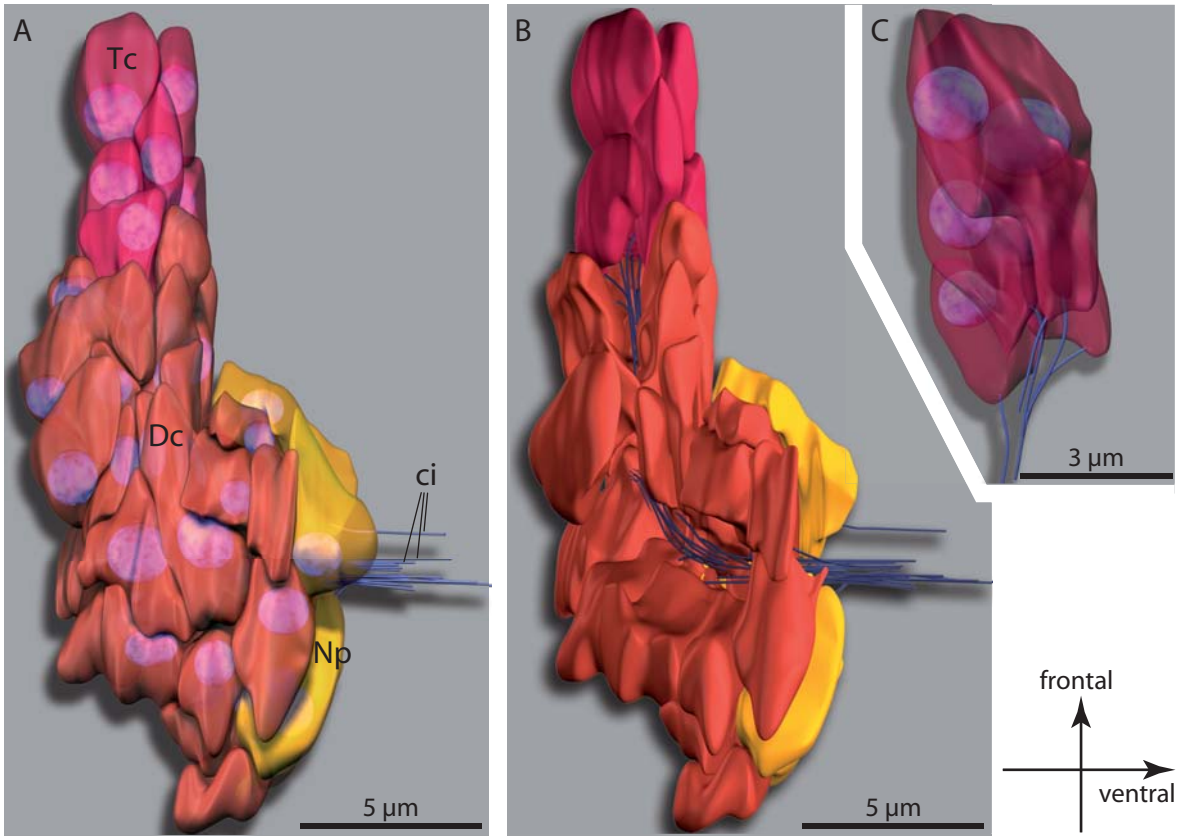

Fig. 10: 3D reconstruction of the protonephridium in *P. ovalis*, taken from serial ultrastructural sections. **A** The protonephridium is composed of nephroporus (*Np*), an angulate duct (*Dc*), as well as proximal terminal cells (*Tc*). All cells are outlined semi-transparent in order to show the nuclei. **B** same illustration as A, some cells are hidden, to show the course of the duct lumen with the cilia of the termianl und duct cells. **C** Terminal complex of the protonephridium, showing the five terminal cells.

the visceral ECM and are connected to the matrix by hemidesmosomes (Fig. 8 C). The cells on the visceral side have acquired polarity and form a layer of interconnected monocilitated epithelio-muscle cells, which contain bundles of basally situated myofilaments (Fig. 7 B). The apical surface is smooth, some having cilia as their only surface extension (Fig. 8 B). Each cell possesses slender filamentous processes, which may overlap with adjacent cells. These processes are connected to processes from neighbouring cells by adherens junctions (Fig. 8 C). Their nuclei are spherical and relatively large in comparison to the size of the cells. The cells on the visceral side are anchored in the periintestinal matrix by cytoplasmatic protrusions (Fig. 7 A).

Two blastocoelic spaces reappeared in this larval stage: the first is located in front of the anterior coelomic lumen, between coelom and epidermis, oriented parallel to the longitudinal axis of the larva; the second one is formed lateral to the posterior coelomic anlage. An apical neuropil is present, located ventral of the anterior blastocoelic space. This apical neuropil is sending three processes, running subepidermally alongside the coelom: two are

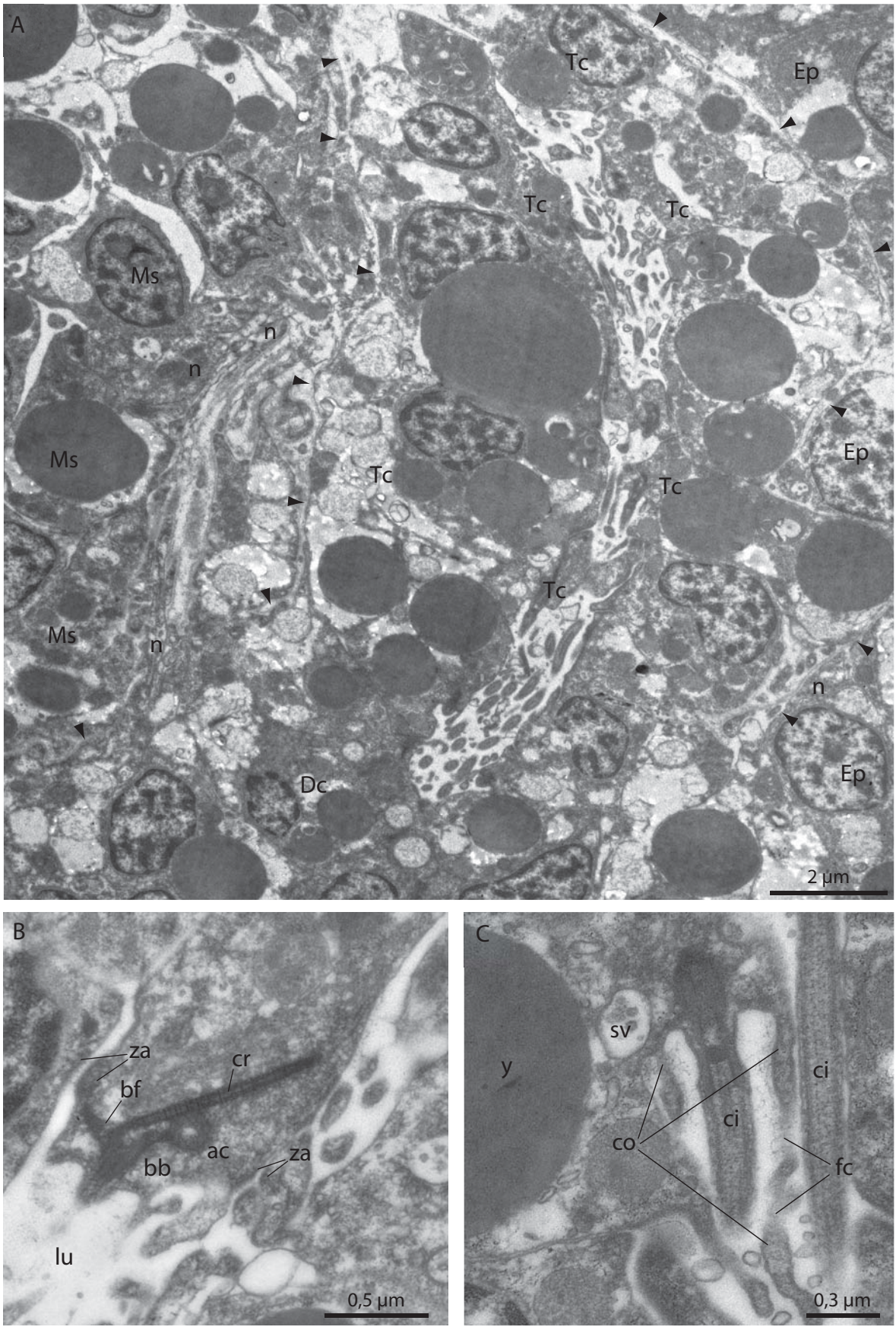
A
Tc
Ep
Tc
Tc
Ms
n
n
Ms
Tc
Tc
Ep
Tc
Ms
n
n
Ep
Dc
2 µm
B
za
cr
bf
ac
za
bb
lu
0,5 µm
C
sv
y
ci
ci
co
fc
0,3 µm

running lateral and ventral to the posterior to the posterior margin of the second blastocoel; the third process is short, running dorsad, covering parts of the anterior blastocoel.

Nephridia in the larva of *P. ovalis*

The nephridia develop from an ectodermal invagination on the lateral side (Fig. 5 A) about the time when the proctodeum. They are located on both sides of the procotodeum. Originating from the nephroporus on the ventro-lateral side, the nephridia extend dorso-centrad and are pushed into the solid mesodermal anlage. After the anterior coelom is formed, each nephridium is located posterior to the opening of the anus in the groove build by the midventral extension of the body (Fig. 9). Each nephridium is composed of three different sections: terminal region, nephroporus region and a duct connecting the terminal and the nephroporus regions. The nephroporus opens on the ventrolateral side of the larval body (Fig. 9). Starting from the nephroporus, the duct runs perpendicular to the outer surface in the form of a straight tube. It bends after 7 µm by 90 degree thus running parallel to the longitudinal axis of the larva, between epidermis and mesoderm, embedded in the epidermal cell sheet (Fig. 12). After another 13 µm the duct ends in a complex of several terminal cells, which are covered by ECM and border the mesodermal anlage on the proximal side of the larva and the epidermis on the lateral side (Fig. 11). The entire length of the nephridium is 25 µm.

Solenocytes

The terminal complex is formed by six monociliary cells. The cells are basally interlocked with the ECM of the mesoderm. Each terminal cell is surrounded by ECM. The perikarya of the terminal cells possess a diameter of 4-5 µm and the terminal cells are bulb-shaped appearance with a cylindrical neck facing towards the lumen of the nephridial canal (Fig. 10). The nucleus is spherical or approximately of spherical form – due to the large yolk vesicles found in the perikaryon - and located central in the perikaryon (Fig. 11). Each cilium is located pericentrally on the apical side in each of the terminal cells; it protrudes

Fig. 11: Terminal complex of the protonephridium in the larva of *P. ovalis*. **A** Longitudinal section through the terminal complex. The terminal cells (*Tc*) are pairwise arranged lining the lumen (*lu*) of the protonephridium. The protonephridium is enclosed by ECM (*arrowheads*), and is embedded between the mesodermal (*Ms*) and epidermal cell (*Ep*) sheets. **B** Longitudinal section through cilium (*ci*), basal structures and microvilli of the terminal cell. **C** Longitudinal section through the proximal part of the filter of the terminal cell. Note the filter clefts (*fc*) in the collar (*co*). *ac:* accessory centriol; *bb:* basal body; *bf:* basal foot; *cr:* ciliary rootlet; *n:* neuropil; *sv:* secretory vesicle; *y:* yolk; *za:* zonula adherens.

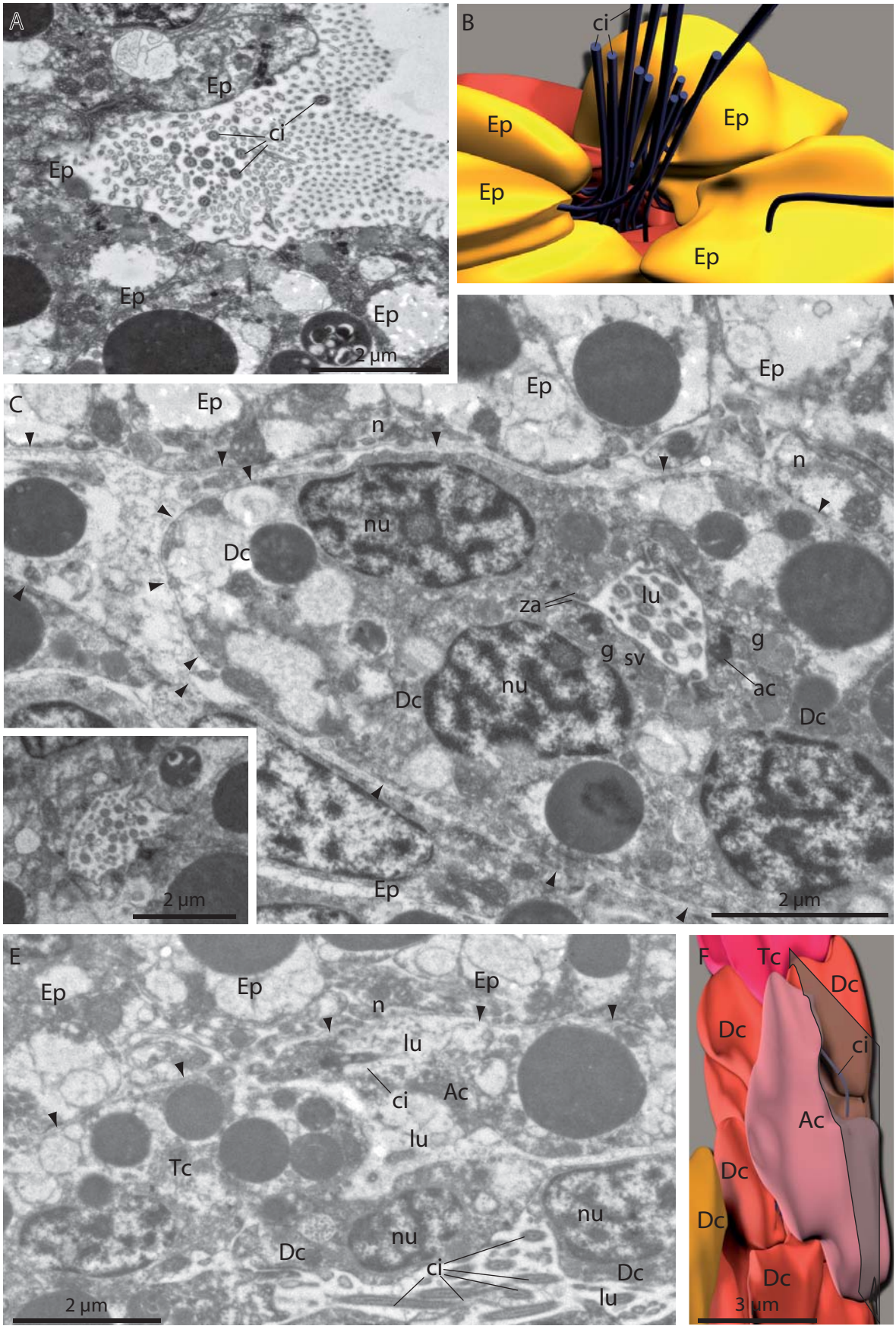
A
Ep
ci
Ep
Ep
Ep
2 µm
B
ci
Ep
Ep
Ep
Ep
C
Ep
n
nu
Dc
Ep
Ep
n
za
lu
g
sv
g
ac
nu
Dc
Dc
2 µm
Ep
2 µm
E
Ep
Ep
Ep
n
lu
ci
Ac
lu
Tc
nu
nu
Dc
ci
Dc
lu
2 µm
F
Tc
Dc
Dc
ci
Ac
Dc
Dc
Dc
3 µm

into the protonephridial lumen and extends distally into the nephridial duct (Fig. 11 B, C). The cilia range in length from 3.2 µm up to 4.9 µm with an average length of 4.2 µm (n=6). The axoneme of the cilium is attached to the basal body to which an accessory centriole is orientated at an angle of 30° to the axis of the cilium. A ciliary rootlet extends deep into the cell with a length of 1 µm and an angle of 30° to the axis of the cilium (Fig. 11 B). A basal foot is attached perpendicular to the basal body on the opposite side of the accessory centriole (Fig. 11 B). Rod-like cytoplasmatic extensions encircle the cilium at intervals of 0.3 µm and follow its way down the nephridial lumen for ca. 3 µm. The 60 to 110 nm thick rods are interwoven and form a rigid collar with small filter clefts between the bars (Fig. 11 C). The clefts are closed by a fine extracellular material, the diaphragm. The space between cilium and collar contains several electron light staining microvilli, which are 0.4 µm long and 0.2 µm wide. They are extensions of the apical surface of the terminal cell. Later in development, the terminal complex elongates, bringing the terminal cells in a pair wise serial arrangement alongside the protonephridial lumen (Fig. 11 A).

Accessory cell

One of the terminal cells differs from the other terminal cells. This accessory cell is located between the terminal cells and the duct cells (Fig. 12 E, F). It differs from the other terminal cells by having the cilium outside the filter and the filter is formed lateral on the cell body. A small space, tapered by ECM, which is continuous with the nephridial lumen, is located between the accessory cell and the epidermis (Fig. 12 E, F). The short cilium reaches into this space (Fig. 12 F).

Fig. 12: Protonephridium of *P. ovalis*. **A** TEM micrograph of the nephroporus. **B** Reconstruction of nephroporus region build by five Epidermal cells. **C** Proximal part of the nephridial duct. **D** Central part of the duct. Each cilium is surrounded by 11 microvilli. **E** Accessory cell (*Ac*) with a single cilium (*ci*) in the blastocoelic space (*bl*) between protonephridium and ECM (*arrowheads*) of the epidermal cells *Ep*. **F** Reconstruction of the position of the accessory cell in the protonephridium. *Dc:* duct cell, *nu:* nucleus, *n:* neuropil, *Tc:* terminal cell.

Nephridial duct

The straight channel is build up by 24 cells, including the nephroporus region, which itself is composed of five cells (Fig. 10, 12). Three different regions can be discriminated in the nephridial duct, as indicated by the arrangement of the cilia (Fig. 10 B). Five monociliary cells constitute the proximal region of the channel which is bordering the terminal cell complex. Unlike the terminal cells and the other duct cells, the apical surface of the duct cells is smooth; no microvilli are present (Fig. 12 C). The cilia have a length between 5 and 6.3 µm with an average length of 5.7 µm (n=17). The nuclei are located central in the cells. Several secretory vesicles are found in the cytoplasm of the cells (Fig. 12 C). The central part of the duct consists of 6 cells. Here the duct bends by 90° towards the surface. The cilia range in length from 6 up to 9 µm, 7 µm in average. Each cilium is surrounded by 9 microvilli (Fig. 12 D). The nuclei are located basally in the cells. Distal, the duct is build up by 8 monociliary cells, with 9 microvilli surrounding each cell. This distal region includes the five cells forming the opening of the duct to the exterior, the nephroporus (Fig. 12 A, B). There is no cytological difference between these cells forming the nephroporus, the duct cells and the epidermal cells.

Origin of the coelom in *Phoronis muelleri*

Overview

Shown here is the early development of *P. muelleri* with emphasis on the origin of the first mesodermal cells. First mesoblasts could be observed during initial gastrulation, when the vegetal side of the embryo of *P. muelleri* starts to invaginate (Fig. 13). They appear around the invaginating cells, on the rim of the prospective blastopore. In later stages they could be observed in several places in the blastocoelic space lying on the basal lamina that surrounds the blastocoelic space (Fig. 14). By the time the proctodeum connects to the archenteron, these cells acquire polarity and settle on the basal lamina of the ectoderm in the prospective episphere. They undergo mitosis and form at least two separate strands of cells, in which individual cells are interconnected to each other by apical adherence junctions. Other mesodermal cells can be found in the blastocoelic space of the tentacle region (Fig. 14). Later the primordium of the protonephridial anlage invaginates from ectodermal cells at the junction of the proctodaeum with the ectoderm (Fig. 15). The epithelialization of the mesodermal cells in the blastocoelic space of the episphere has progressed in this stage, although the individual strands do not form a complete epithelium (Fig. 15 B).

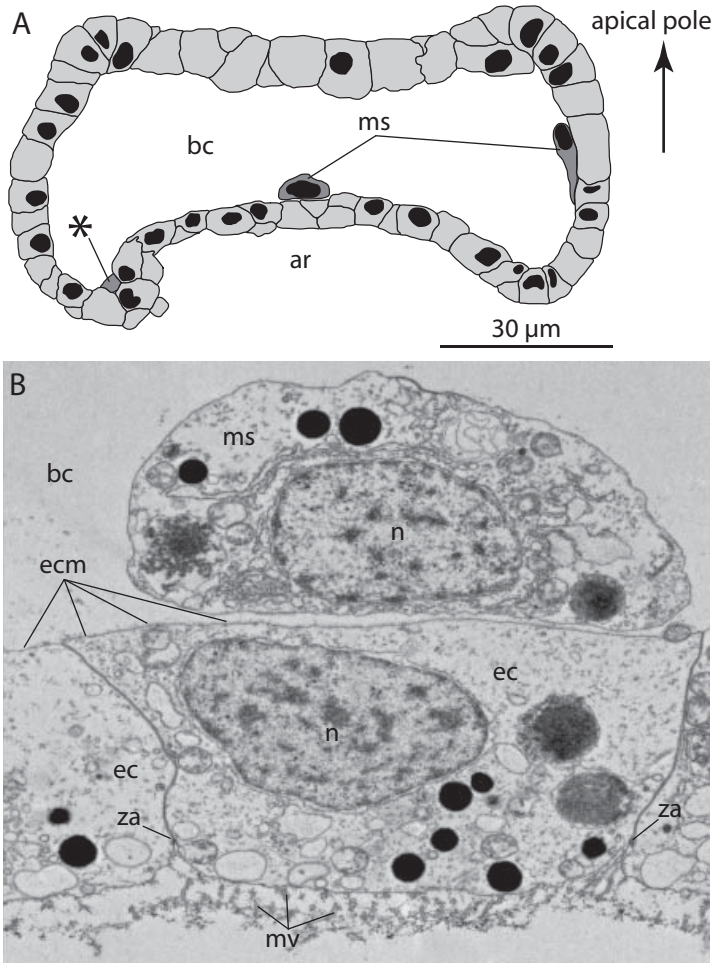

Fig. 13: *P. muelleri* 30h old. **A** Schematic drawing copied from TEM micrograph. Light gray shaded cells represent ectodermal cells, dark shaded cells are mesoblasts (*ms*) in the blastocoel (*bc*), nuclei of cells are black shaded. Three single mesoblasts could be observed in this early gastrula stage, one seems to be just migrated from the ectodermal lining (*asteriks*) from the corner around the blastoporus (*b*). **B** Single mesoblast lying on the roof of archenteron. The ectodermal cells (*ec*) are connected to each other by apical zonula adherens (*za*) and the apical surface is is drawn out into numerous microvilli (*mv*). Note: there is no epithelialization of the mesoblast nor any desmosomes connecting the mesoblast to the underlying basal lamina (*ecm*) of the ectoderm. *ar*: archenteron, *n*: nucleus.

Gastrula stage

The embryo at the beginning of gastrulation, 30h PF, is of ovoid shape. Gastrulation starts with the invagination of the vegetal side, forming the archenteron with the lateral lips narrowed, leaving the blastopore opening. The ectodermal cells are interconnected by apical adherens junctions and rest on basal lamina, thus forming a true epithelium at the moment of gastrulation. At the apical pole the ectodermal cells are club-shaped, the thickened basal parts overlapping each other, giving the epithelium a double layered appearance in longitudinal sections (Fig. 13 A). The cells on the lateral sides are cuboid, the nucleus small

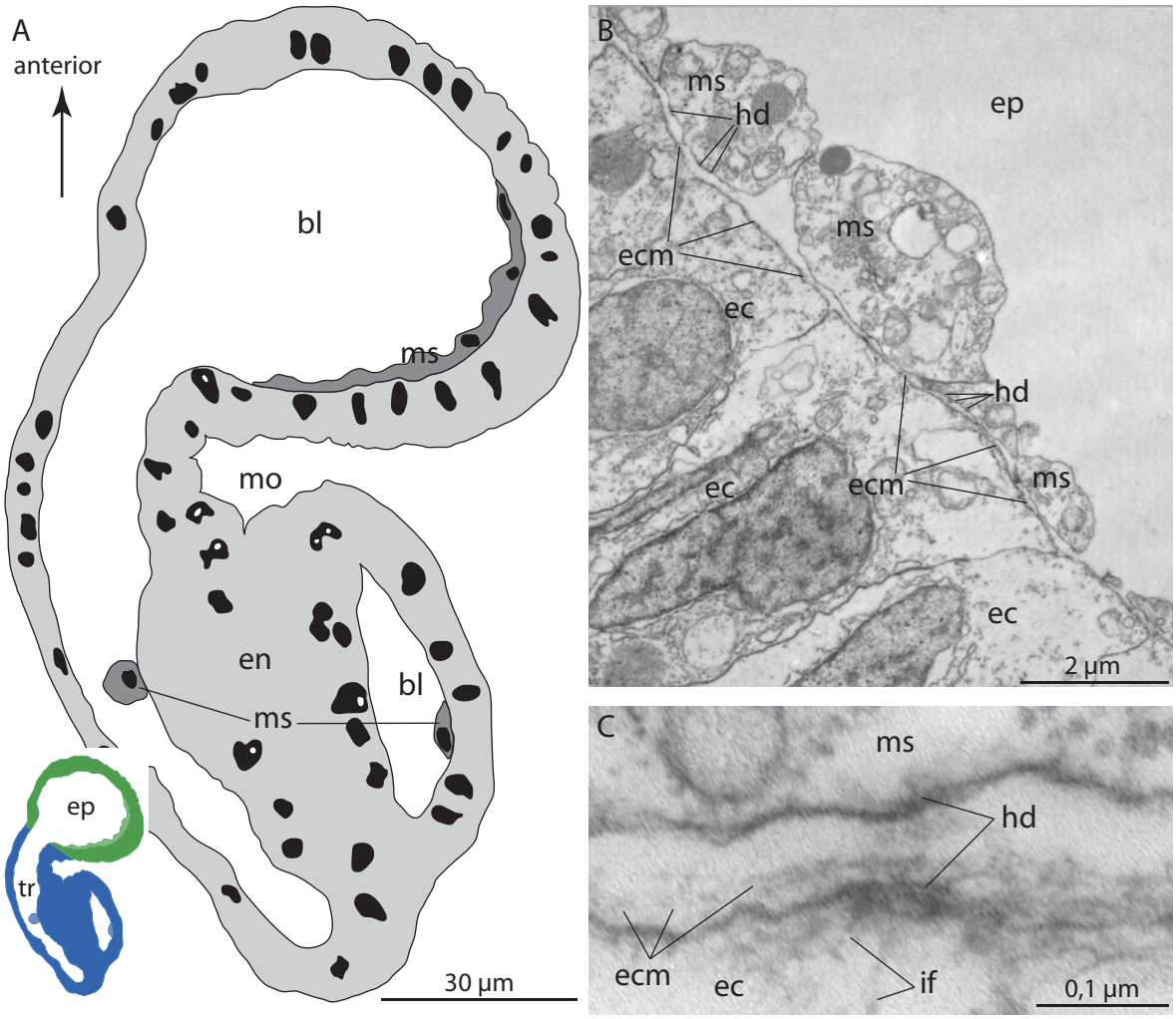

Fig. 14: *P. muelleri*, 3 days old. **A** Longitudinal section drawn from TEM micrograph. Mesodermal cells (*ms*) in the blastocoelic space (*bl*) of the episphere (*ep*) started to form an epithel. The blastocoelic space of the tentacle region (*tr*) contains some single mesodermal cells. Inlay: regionation in *P. muelleri*, colored to indicate position of episphere and tentacle or collar region, both separated by mouth opening. **B** Detail of the mesodermal cells settling on the basal lamina (*ecm*) of the blastocoel in the episphere. **C** Hemidesmosome (*hd*) connecting mesoderm cell and ectoderm cell (*ec*) to the basal lamina. (*if*) intermediar filament.

and spherical. They contain globular electron dark vesicles as well as numerous electron black yolk vesicles.

Single cells appear inside the blastocoelic space. They seem to originate from the edges around the blastopore (Fig. 13 A *asteriks*). They can be found on numerous places throughout the blastocoelic space, but always lying on the basal lamina tapering the blastocoelic space, but not attached to it by discernible junctional complexes (Fig. 13).

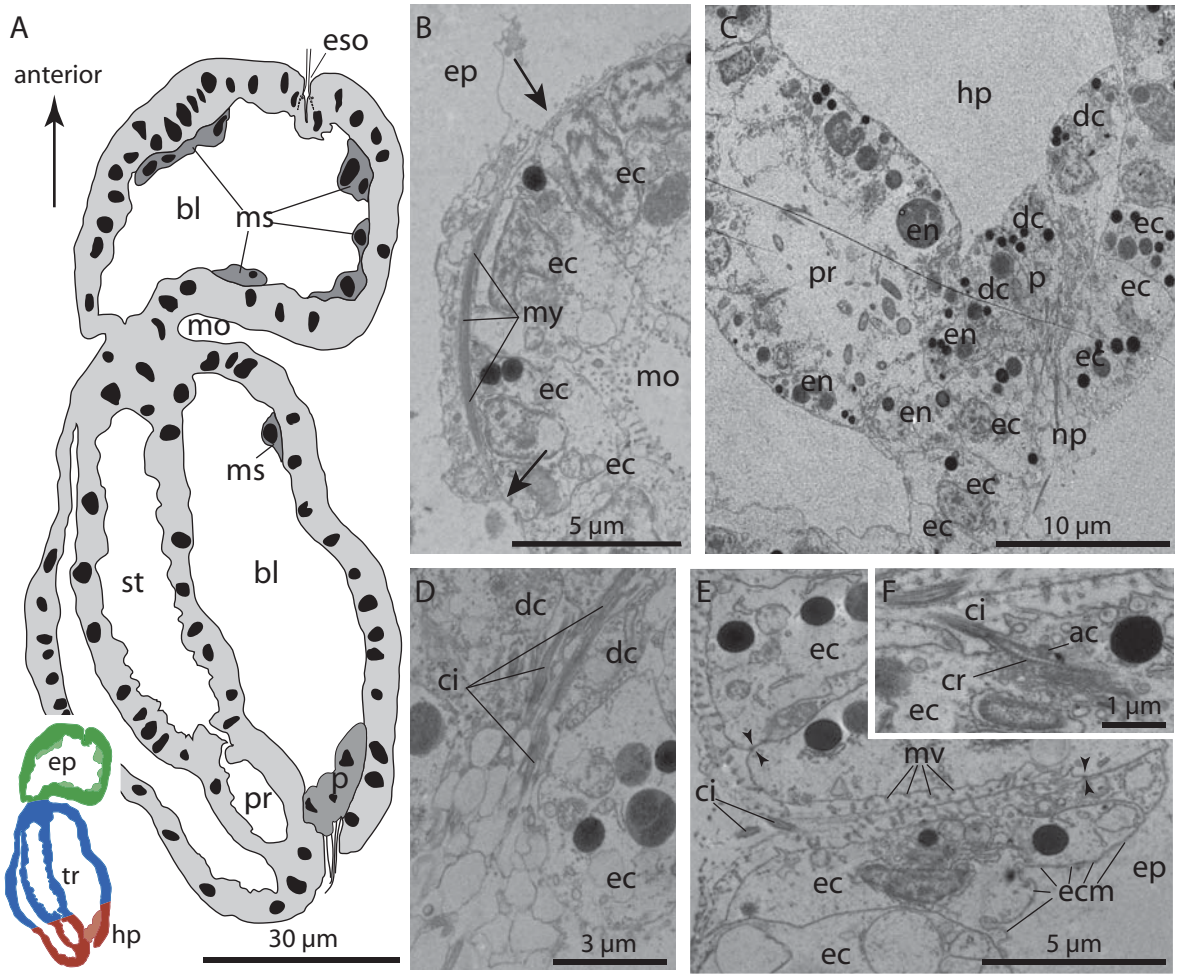

Fig. 15: *P. muelleri*, 5½ days old. **A** Longitudinal section drawn from TEM micrographs. The stomodeum (*st*) fuses with the proctodeum (*pr*) and the nephridial anlage (*p*) forms in front of the proctodeum on the posterior side. In front of the apical plate the eversible sense organ (*eso*) is developed. Mesodermal cells (*ms*) settle on the basal lamina of the blastocoelic space in the episphere (*ep*). Single mesodermal cells taper the blastocoelic wall of the tentacle region (*tr*). Inlay: regionation in *P. muelleri*. Colors represent episphere (green), tentacle or collar region (blue) and hyposphere *hp* (red) **B** Some mesodermal cells in the episphere have already differentiated into myoepithel cells, like this cell lining the blastocoelic space around the mouth opening (*mo*) with basal myofibrils (*my*). Note: the lining of cells is incomplete (*arrow*). **C** Detail of the nephridial anlage formed by three duct cells (*dc*) postero-lateral of the proctodeum. **D** Longitudinal section through the developing protonephridial anlage. **E** Eversible sense organ consisting of several monociliated cells which can be evaginated. The cells are interconnected by apical zonula adherens (*arrowheads*). **F** Detail of the cell of the eversible sense organ. *ac*: accesory centriole, *al*: apical plate, ci: cilium, *cr*: ciliary rootlet, *ec*: ectodermal cell, *np*: nephroporus, *mv*: microvilli.

Young larva after gastrulation

After gastrulation, ca. 2 h PF the axis of the larvae has bent 90 degree (Fig. 14 A); the apical pole has moved lateral, thus becoming the anterior tip of the developing larva, the blastopore opens on the ventral side with the opening shifted inwards forming the larval mouth opening (Fig. 14 A). The archenteron bends posterior and extends into the stomo-

deum, which runs towards the posterior pole of the larva, opposite to the new apical side. The young larva can be readily divided into two distinct regions; the area anterior to the posterior bending of the archenteron forms the episphere, which enlarges and overhangs the mouth, thus forming a vestibule anterior to the mouth opening (Fig. 14 A), whereas the posterior area behind the mouth opening forms the future tentacular or collar region. The blastocoelic space is undivided and enclosed by the epidermis, which consists of columnar cells in the episphere with a height of 6 to 10 µm on the ventral and apical sides. The epidermis on the dorsal side is build by small cuboid cells, between 2.5 and 4 µm in height. The blastocoelic space is lined by a delicate basal lamina which is ca. 30 nm thin (Fig. 14 C). In the blastocoelic space of the episphere the mesoblasts have undergone mitosis and are interconnected by adherens junctions, and are connected to the basal lamina by hemidesmosomes, thus forming an incomplete epithelial lining on the posterior wall (Fig. 14 B). Single mesoblasts, not connected to the basal lamina are found in the blastocoelic space lining the wall of the stomodeum and the ventral wall of the tentacular blastocoel (Fig. 14 A).

Two lobed larva

In larva 5 d PF the proctodeum is formed on the posterior side. Now the larva could be divided in the anterior episphere, the tentacular region containing the stomodeum and the tentacular anlagen, and the posterior hyposphere or prospective trunk region with the proctodeum (Fig. 15 *inset*). The tentacular region is now characterized by thickened epidermal cells, which constitutes the anlagen of the larval tentacles (Fig. 15 A). More mesoblasts undergo mitosis and form a strand of epithelial cells lining the basal lamina of the blastocoel of the episphere. Likewise a second epithel could be observed directly underneath the apical plate. Some of the cells in the blastocoelic space in the episphere have differentiated and form a ring of myoepithel cells around the mouth opening (Fig. 15 B) as well as a patch of cells underneath the apical plate. Solitary mesoblasts could still be found on the ventral side in the tentacular blastocoel. A mass of cells is proliferated from the epidermal cells at the edges in front of the proctodeum in the hyposphere. These cells form the primordium of the protonephrial anlage (Fig. 15 C). This protonephridial anlage consists of several cells with long cilia, which reach through a small opening in the ectodermal sheet of cells to the outside, thus forming the nephroporus (Fig. 15 D-F). At the same time as the protonephridia are formed, the eversible sense organ in front of the apical plate is build by cells, that are invaginated under the ectodermal epidermis cells, sending their cilia to the outside (Fig. 15 D-F).

Discussion

Origin of the coelom in Phoronida

In the present thesis, the larval development of *P. ovalis* and *P. muelleri* with emphasis on the origin of the mesoderm is described. In the blastula of *P. ovalis* isolated cells were found in the blastocoel. These cells were undifferentiated and - in the larval stage examined - formed a cluster of eight cells, bordering the vegetal side of the blastocoelic space. One single cell could be observed inside the blastocoelic space. Based on these observations, two scenarios for the origin of the mesoderm in *P. ovalis* are conceivable: Firstly, cells could delaminate from the vegetal epithelial blastomeres during the initial stage of gastrulation, as was for instance described by Ikeda (1901) for *P. ijimai*, or, secondly, the cells could migrate from the line of archenteral cells near the blastopore and aggregate on the vegetal side of the blastocoelic space. This latter case has been observed by Zimmer (1964, 1980) in *P .ijimai*, as well as in *P. muelleri* (Herrmann 1986). Cell tracing experiments conducted on *P. ijimai* by Freeman & Martindale (2002), indicate that the mesodermal cells originate from the ectodermal or endodermal cells at the border between the prospective pharynx/ intestine and the mouth or anus. In the present study no signs of cell migration have been found in stages after the gastrula stage in *P. ovalis* and *P. muelleri*. Mesodermal cells migrate from the cells around the future blastopore opening during gastrulation into the blastocoelic space in both species. Either they form a compact mass of cells like in *P. ovalis*, or they become amoeboid and migrate into the blastocoelic space like in *P. muelleri*.

The coelomic lumen is formed by schizocoely and polarization of the compact mesodermal cell mass in *P. ovalis*. In the case of the anterior coelomic cavity, the coelomic lumen forms by mitosis of isolated mesenchymatous cells resting on the basal lamina and forming fragments of epithelial linings in the blastocoel. The fate of these fragmentary epithelial pieces in the anterior coelom in *P. muelleri* has not been traced further in the present study, but, according to studies of Bartolomaeus (2001) on the same species, they form a complete lining of myoepithelial cells, thus obliterating the blastocoelic space in the tentacle region, turning the lumen into a complete coelom. The myoepithelial cells in the episphere of *P. muelleri* as well as *P. pallida* forming fragments of epithelial linings remain fragmented during the entire larval life (Bartolomaeus 2001, Santagata 2002: Fig. 2 B). The blastocoelic space in the episphere persists and is filled by an amorphous gel-like matrix (Bartolomaeus 2001), which probably stabilizes the episphere.

This kind of mesoderm origin from isolated cells is found in other taxa as well: In embryos

of *Asterina pectinifera* (Echinodermata) the animal blastomeres of the eight-cell stage give rise to the anterior ectoderm and the stomodeum. The vegetal cells give rise to the posterior ectoderm and the mesendoderm (Kominami 1983, Maruyama & Shinoda 1990). In *Ptychodera flava* (Hemichordata) the Brachyury gene expression occurs during gastrulation in the future anal and oral regions of the gut (Peterson & Eernisse 2001). The coelom originates from cells that delaminate from the wall of the gut and merge together to form a solid mass of cells (Peterson & Eernisse 2001). In *Thulinia stephaniae* (Eutardigrada) examined by Hejnol & Schnabel (2004), the gastrulation starts with immigration of single blastomeres. Mesoderm and endoderm precursors proliferate after gastrulation. After they enter the blastocoel, they adhere to the inside of the outer ectodermal layer, on which they migrate to their final position. During this migration, the cells proliferate and form bands along the left and right side of the prospective pharynx and midgut (Hejnol & Schnabel 2004).

Homology of *P. ovalis* larva with the Actinotrocha

According to different authors, different numbers of coelomic spaces are present in the phoronid larvae: in *Phoronopsis harmeri* three (Temereva & Malakhov 2006), in *P. ijimai* (Zimmer 1980), and in *P. muelleri* (Bartolomaeus 2001) two, as well as in *P. ovalis* two (this study). In order to understand this discrepancy, the correlation of the larva of *P. ovalis* with the other phoronid larva of the actinotrocha type needs to be shown. Although the larva of *P. ovalis* does not resemble an actinotroch larva based on external appearance, Silén (1952) already suggested corresponding features in both larval types by comparing only the outer morphology. He suggested the anterior ventral rim around the mouth opening to be homologous to the actinotroch episphere; the ventral extensions should correspond to the actinotroch trunk. The present study provides additional information, which helps in finding correlated features in both larval types. In order to accomplish this, a common fixed point, present in both larval types, needs to be found. After that, the differing morphological characters can be compared.

In the larva of *P. ovalis* an anterior neuropil is formed with a coelomic space located posterior to this neuropil, and a small blastocoelic space between coelom and neuropil. This anterior coelom encircles a wide midventral mouth opening and pharynx. Separated from the anterior coelom a second compact coelomic anlage is formed which covers the anlage of the intestine. Lateral to the posterior coelomic anlage, a small blastocoelic space is formed. Posterior to this blastocoelic space, between cell sheets of epidermis and mesoderm, the larval protonephridia are formed on both sides of the anus. Protonephridia are present in both larval types, and can therefore be used as fixed point for the detection of homologous

features in the larva of *P. ovalis* and the actinotroch larva. An anterior neuropil is present in both larval types, as well as a blastocoelic space in the region of the trunk coelom in the actinotroch larva and in the region of the posterior mesoderm of *P. ovalis*. This apical neuropil provides a second fixed point. The nephridial duct runs through the trunk coelom in larva of *P. muelleri* (Bartolomaeus, 1989), whereas in *P. ovalis* larva the duct runs alongside the posterior mesoderm. In the larva of *P. muelleri* the tentacles are filled by an amorphous matrix (Bartolomaeus 2001); adult tentacles are added shortly before metamorphosis as buddings below the larval tentacles. The tentacle coelom is formed by fluid accumulation in the subepidermal double layered myoepithel at the bases of the buds of the adult tentacles (Bartolomaeus 2001). In the larvae of *P. ovalis* there are no larval or adult tentacles present until metamorphosis (Silén 1952). The gut of the actinotroch larva is straight; the anus of the *P. ovalis* larva is located just posterior to the mouth opening, forcing the developing intestine to bend like an U. With this knowledge in hand, the homologies in the larva of *P. ovalis* with the actinotroch larva are as follows:

- The anterior coelom of the *P. ovalis* larva corresponds to the tentacle coelom in front of the protonephridia. This coelom extends anterior until the apical neuropil.
- An expanded episphere, overhanging the mouth opening, like in the actinotroch larva, is not present.
- The trunk coelom of the actinotroch larva corresponds to the posterior coelom in *P. ovalis* larva.
- The ventral extension of the *P. ovalis* larva has no correspondence in the actinotroch larva. Later in development the ventral extensions becomes elongated and seems to fuse with the posterior body, according to the drawings in Silén (1952).

The condition in the ground pattern of Phoronida

If we return now to the question regarding the number of coelomic spaces in the larva of the Phoronida: There are two coelomic spaces or anlagen of coelomes found in the larva of *P. ovalis* and *P. muelleri*. The future episphere and hyposphere are continuous in early larva of *P. muelleri*, and it is likely that the mesenchymatous lining, tapering the blastocoelic space of the hyposphere, originates from the same source (see above) as the epithelium of the anterior coelom. The coelomic lining of the hyposphere in actinotroch larvae of *Ph. harmeri*, *P. ijimai*, and *P. muelleri* is formed when the trunk of the larva elongates (Zimmer 1980, Bartolomaeus 2001, Malakhov & Temereva 1999). Some authors agree on the findings, that a coelom in the larval hood is formed later in larval life and that it is separated from the tentacle coelom by a complete septum (Zimmer 1980, Malakhov & Temereva

1999). Based on serial ultrastructural sections Bartolomaeus (2001) proved that neither in larval nor adult *P. muelleri* an anterior coelom separate from the tentacle coelom is present. Recent studies on the development of *Ph. harmeri* revealed a single coelomic cavity in the preoral hood of the larva, just underneath the apical plate (Temereva & Malakhov 2006). *P. ijimai* has a transitory coelomic space in the preoral hood, which is completely obliterated after the larva breaks free from the parental tube (Zimmer 1980).

Two scenarios can be responsible for the discrepancies reported on the condition of the number of coeloms in the Phoronida:

1. An actinotroch larva with three coelomic cavities was present in the stemlineage of the Phoronida.
2. An actinotroch or a larva similar to the actinotroch larval type with one coelomic anlage, and two coelomic cavities later in larval life was present in the stemlineage of the Phoronida.

The first scenario is supported by the results for *Ph. harmeri* (Temereva & Malakhov 2006); *P. ijimai* (Siewing, 1973) and *P. muelleri* (Siewing 1974b, Herrmann 1986). Although Siewing (1974a, 1980b), Herrmann (1997), and recently Temereva & Malakhov (2006) interpret their results as a strong support for the archicoelomate theory, other authors see no support for this theory in phoronid anatomy (Zimmer 1980, Bartolomaeus 2001, this study) or in the related outgroups of the phoronids, the Brachiopoda. The coelom in *Novocrania anomala* (Müller, 1776) develops out of a single coelomic anlage, which becomes divided into an anterior and posterior compartment later in larval life (Grobe 2000, Grobe, Lüter & Bartolomaeus in prep.). In the three-lobed developmental stages of the articulate brachiopods, *Calloria inconspicua* (Sowerby, 1846) and *Notosaria nigricans* (Sowerby, 1846), a compact mesoderm surrounding the endoderm is present (Lüter 1998, 2000). Coelomogenesis is accomplished by fluid accumulation between the double layered mesodermal cells (Lüter 1998, 2000). Thus, in these latter taxa the coelom develops also out of a single anlage. These conditions in the brachiopods support the hypotheses that a larva with a coelom that develops out of one anlage and becomes later divided into two compartments is found in the stemlineage of the Brachiopoda. Thus, the plesiomorphic condition of coelom formation in Brachiopoda closely resembles the condition observed in *P. ovalis*, where also two coelomic compartments develop from a single ontogenetic rudiment. Because Phoronida also share several other similarities with Brachiopoda, it can be hypothesized that the mode of coelom formation in the stem lineage of Phoronida was inherited without modifications from the common ancestor of Brachiopoda and Phoronida. These interpretations also support a basal position of *P. ovalis* in the phoronid clade. This latter conclusion is further supported by the lecithotrophic development of *P. ovalis*, because a lecithotrophic larva

likely represents the groundpattern condition of the brachiopods (Haszprunar *et al.* 1995, Lüter 1998, 2000). The remaining phoronids have an entirely planctotrophic development, or, in brooding species, a planctotrophic larval phase follows an initial lecithotrophic phase in early larval life, that lasts until the first functional tentacles are formed and the larva breaks free from the parental tube (Silén 1952, Emig 1974, 1977).

Literature

Bartolomaeus, T. (1989): Ultrastructure and relationship between protonephridia and metanephridia in *Phoronis muelleri* (Phoronida). Zoomorphology 109: 113-122.

Bartolomaeus, T. (2001): Ultrastructure and formation of the body cavity lining in *Phoronis muelleri* (Phoronida, Lophophorata). Zoomorphology 120: 135-148.

Brooks, W. K. & Cowles, R. P. (1905): *Phoronis architecta*: its life history, anatomy and breeding habits. Mém. Nat. Acad. Sci. Washington 10: 75-111.

Caldwell, W. H. (1885): Blastopore, mesoderm, and metameric segmentation. Q. J. Micr. Sci. 25: 15-28.

Crawford, B. (1989): Ultrastructure of the basal lamina and its relationship to extracellular matrix of embryos of the starfish *Pisaster ochraceus* as revealed by anionic dyes. J. Morph. 199: 349-361.

de Selys-Longchamps, M. (1907): Phoronis. Fauna und Flora des Golfes von Neapel 30: 1-280.

Emig, C. C. (1971): Remarques sur la systematique des Phoronidea. X. Notes sur l'ecologie, la morphologie et la taxonomie de *Phoronis ijimai* et *Phoronis vancouverensis*. Mar. Biol. 8: 154-159.

Emig, C. C. (1974): Observations et discussions sur le développement embryonnaire des Phoronida. Z. Morph. Tiere 77: 317-335.

Emig, C. C. (1976): Phylogenèse des Phoronida, les Lophophorates et le concept des Archimerata. Z. Zool. Syst. Evol.-Forsch. 14: 10-24.

Emig, C. C. (1977): The embryology of Phoronida. Amer. Zool. 17: 21-38.

Emig, C. C. & Siewing, R. (1975): The epistome of *Phoronis psammophila* (Phoronida). Zool. Anz. 194: 47-54.

Freeman, G. & Martindale, M. Q. (2002): The origin of mesoderm in phoronids. Dev. Biol. (Orlando) 252: 301-311.

Grobe, P. (2000): The ultrastructure of the larva of Neocrania anomala (Brachiopoda). Zoology 103: 101.

Gruhl, A.; Bartolomaeus, T. & Grobe, P. (2005): Fine structure of the epistome in *Phoronis ovalis*: significance for the coelomic organization in Phoronida. Inv. Biol. 124 (4): 332–343.

Haszprunar, G., L. Salvini-Plawen & R. M. Rieger (1995): Larval planktotrophie - a primitive trait in the Bilateria? Acta Zool. (Stockh.) 76: 141-154.

Hejnol, A. and Schnabel, R. (2004): The eutardigrade *Thulinia stephaniae* has an indeterminate development and the potential to regulate early blastomere ablations. Development 132: 1349-1361.

Herrmann, K. (1980): Die archimere Gliederung bei *Phoronis muelleri* (Tentaculata). Zool. Jb. Anat. Ontog. Tiere 103: 234-249.

Herrmann, K. (1986): Die Ontogenese von *Phoronis mülleri* (Tentakulata) unter besonderer Berücksichtigung der Mesodermdifferenzierung und Phylogenese des Coeloms. Zool. Jb. Anat. Ontog. Tiere 114: 441-463.

Herrmann, K. (1997): Phoronida. In: Microscopic Anatomy of Invertebrates, Harrison, F. W. & Woollacott, R. M. (eds.). Vol. 13: Lophophorates, Entoprocta and Cycliophora Wiley-Liss, New York, 207-235.

Hyman, L. H. (1959): Phoronida. In: The Invertebrates - Smaller Coelomate Groups Vol. 5 McGraw-Hill, New York, 228-274.

Ikeda, I. (1901): Observations on the development, structure and metamorphosis of Actinotrocha. J. Coll. Sci. Imp. Univ. Tokyo 13: 507-592.

Kominami, T. (1983): Establishment of embryonic axes in larvae of the starfish, *Asterina pectinifera*. J. Embryol. Exp. Morphol. 75: 87-100.

Kowalewsky, A. (1867): Anatomy and history of development in *Phoronis*. Bull. Acad. Sci. St. Petersburg 11: 1-14.

Lüter, C. (1998): Zur Ultrastruktur, Ontogenese und Phylogenie der Brachiopoda. Dissertation, Universität Göttingen. Cuvillier Verlag, Göttingen.

Lüter, C. (2000): The origin of the coelom in Brachiopoda and its phylogenetic significance. Zoomorphology 120: 15-28.

Malakhov, V. V. & Temereva, E. N. (1999): Embryonic development of the phoronid *Phoronis ijimai* (Lophophorata, Phoronida): Two sources of the coelomic mesoderm. Dok. Biol. Sci. 365: 166-168.

Maruyama, Y. K. & Shinoda, M. (1990): Archenteron forming capacity in blastomeres isolated from eight-cell stage embryos of the starfish, *Asterina pectinifera*. Dev. Growth & Diff. 32: 73-84.

Masterman, A. T. (1898): On the theory of archimeric segmentation and its bearing upon the phyletic classification of the coelomata. Proc. R. Soc. Edinb. 22: 270-310.

Masterman, A. T. (1900): On the Diplochorda. III. The early development and anatomy of *Phoronis buskii*, McIntosh. Q. J. Micr. Sci. 43: 375-418.

Peterson, K. J. & Eernisse, D. J. (2001): Animal phylogeny and the ancestry of bilaterians: inferences from morphology and 18S rDNA gene sequences. Evol. & Dev. 3: 170-205.

Pross, A. (1980): Untersuchungen zur Gliederung von *Lingula anatina* (Brachiopoda). - Archimerie bei Brachiopoden. Zool. Jb. Anat. Ontog. Tiere 103: 250-263.

Reisinger, E. (1972): Die Evolution des Orthogons der Spiralier und das Archicoelomatenproblem. Z. Zool. Syst. Evol.-Forsch. 8: 81-109.

Santagata, S. (2002): Structure and metamorphic remodelling of the larval nervous system and musculature of *Phoronis pallida* (Phoronida). Evol. & Dev. 4: 28-42.

Santagata, S. (2004): Larval development of *Phoronis pallida* (Phoronida): implications for morphological convergence and divergence among larval body plans. J. Morph. 259: 347-358.

Sedgwick, A. (1886): The development of the cape species of *Peripatus*. Part II. Quart. J. Micr. Sci. 26: 175-212.

Siewing, R. (1973): Morphologische Untersuchungen zum Archicoelomatenproblem 1. Die Körpergliederung von *Phoronis ijimai* Oka (Phoronida). Z. Morph. Tiere 74: 17-36.

Siewing, R. (1974a): Gliederung des Phoronidenkörpers. Verh. Dtsch. Zool. Ges. 116-121.

Siewing, R. (1974b): Morphologische Untersuchungen zum Archicoelomatenproblem 2. Die Körpergliederung bei *Phoronis mülleri* de Selys-Longchamps (Phoronida). Zool. Jb. Anat. Ontog. Tiere 92: 275-318.

Siewing, R. (1980a): Das Archicoelomatenkonzept. Zool. Jb. Anat. Ontog. Tiere 103: 439-482.

Siewing, R. (1980b): Körpergliederung und phylogenetisches System. Zool. Jb. Anat. Ontog. Tiere 103: 196-210.

Silén, L. (1954): Developmental biology of Phoronidea of the Gullmar Fjord area (West coast of Sweden). Acta Zool. (Stockh.) 35: 215-257.

Temereva, E. N. & Malakhov, V. V. (2006): The answer to Thomas Bartolomaeus: „Larva of phoronid *Phoronopsis hermeri* Pixell, 1912 has trimeric coelom organisation". Dok. Ak. Nauk 410: 425-429 (in russian).

Zimmer, R. L. (1964): Reproductive biology and development of Phoronida. Ph. D. Dissertation, University of Washington, Washington.

Zimmer, R. L. (1980): Mesoderm proliferation and formation of the protocoel and metacoel in early embryos of *Phoronis vancouverensis*. Zool. Jb. Anat. Ontog. Tiere 103: 219-233.